PCT WORLD INTELLECTUAL PROPERTY ORGANIZATION
International Bureau

INTERNATIONAL APPLICATION PUBLISHED UNDER THE PATENT COOPERATION TREATY (PCT)

(51) International Patent Classification 6 : A61B 6/00 — A1

(11) International Publication Number: WO 99/09887

(43) International Publication Date: 4 March 1999 (04.03.99)

(21) International Application Number: PCT/US98/17886

(22) International Filing Date: 28 August 1998 (28.08.98)

(30) Priority Data:

60/057,801	28 August 1997 (28.08.97)	US
60/066,996	28 November 1997 (28.11.97)	US
60/076,760	3 March 1998 (03.03.98)	US

(71) Applicant: QUALIA COMPUTING, INC. [US/US]; Suite G, 2372 Lakeview Drive, Beavercreek, OH 45431 (US).

(72) Inventors: AMBURN, Elton, P.; 7040 Settlement Way, Dayton, OH 45414 (US). BERKEY, Telford, S.; 2190 Cherokee Drive, London, OH 43140 (US). BROUSSARD, Randy, P.; 6255 Beacon Tree Court, Huber Heights, OH 45424 (US). DESIMIO, Martin, P.; 4770 Appaloosa Trail, Fairborn, OH 45324 (US). HOFFMEISTER, Jeffrey, W.; 291 Towncrest Drive, Beavercreek, OH 45434 (US). OCHOA, Edward, M.; 4114 Medical Drive #21108, San Antonio, TX 78229 (US). RATHBUN, Thomas, F.; 3685 Olde Willow Drive, Beavercreek, OH 45431 (US). ROGERS, Steven, K.; 4017 Emerald Court, South, Beavercreek, OH 45430 (US). ROSENSTENGEL, John, E.; 8949 Cypress Gate, Huber Heights, OH 45424 (US).

(74) Agents: ROSE, Mark, E. et al.; Biebel & French, 35 East First Street, Dayton, OH 45402 (US).

(81) Designated States: AL, AM, AT, AU, AZ, BA, BB, BG, BR, BY, CA, CH, CN, CU, CZ, DE, DK, EE, ES, FI, GB, GE, GH, GM, HR, HU, ID, IL, IS, JP, KE, KG, KP, KR, KZ, LC, LK, LR, LS, LT, LU, LV, MD, MG, MK, MN, MW, MX, NO, NZ, PL, PT, RO, RU, SD, SE, SG, SI, SK, SL, TJ, TM, TR, TT, UA, UG, UZ, VN, YU, ZW, ARIPO patent (GH, GM, KE, LS, MW, SD, SZ, UG, ZW), Eurasian patent (AM, AZ, BY, KG, KZ, MD, RU, TJ, TM), European patent (AT, BE, CH, CY, DE, DK, ES, FI, FR, GB, GR, IE, IT, LU, MC, NL, PT, SE), OAPI patent (BF, BJ, CF, CG, CI, CM, GA, GN, GW, ML, MR, NE, SN, TD, TG).

Published
With international search report.

(54) Title: METHOD AND SYSTEM FOR AUTOMATED DETECTION OF CLUSTERED MICROCALCIFICATIONS FROM DIGITAL MAMMOGRAMS

(57) Abstract

A method, a system for detecting, and displaying clustered micro–calcification in a digital mammogram wherein a single digital mammogram (100) is first automatically cropped (200) to a breast area sub–image which is then processed by means of an optimized difference of a Gaussian filter to enhance the appearance of potential micro–calcification in the sub–image. The potential micro–calcification is threshold, clusters are detected (300), features are computed for the detected clusters, and the clusters are classified (400) as either suspicious or not suspicious by means of a neural network. The locations in the original digital mammogram of the suspicious detected clustered micro–calcification are indicated. The results of the system are optimally combined with a radiologist's observation of the original mammogram by combining the observations with the results after the radiologist has first accepted or rejected individual detections reported by the system.

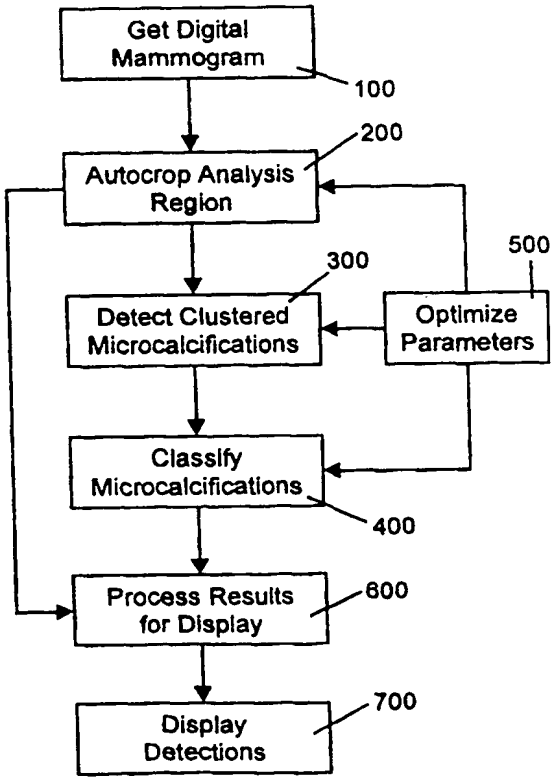

FOR THE PURPOSES OF INFORMATION ONLY

Codes used to identify States party to the PCT on the front pages of pamphlets publishing international applications under the PCT.

AL	Albania
AM	Armenia
AT	Austria
AU	Australia
AZ	Azerbaijan
BA	Bosnia and Herzegovina
BB	Barbados
BE	Belgium
BF	Burkina Faso
BG	Bulgaria
BJ	Benin
BR	Brazil
BY	Belarus
CA	Canada
CF	Central African Republic
CG	Congo
CH	Switzerland
CI	Côte d'Ivoire
CM	Cameroon
CN	China
CU	Cuba
CZ	Czech Republic
DE	Germany
DK	Denmark
EE	Estonia
ES	Spain
FI	Finland
FR	France
GA	Gabon
GB	United Kingdom
GE	Georgia
GH	Ghana
GN	Guinea
GR	Greece
HU	Hungary
IE	Ireland
IL	Israel
IS	Iceland
IT	Italy
JP	Japan
KE	Kenya
KG	Kyrgyzstan
KP	Democratic People's Republic of Korea
KR	Republic of Korea
KZ	Kazakstan
LC	Saint Lucia
LI	Liechtenstein
LK	Sri Lanka
LR	Liberia
LS	Lesotho
LT	Lithuania
LU	Luxembourg
LV	Latvia
MC	Monaco
MD	Republic of Moldova
MG	Madagascar
MK	The former Yugoslav Republic of Macedonia
ML	Mali
MN	Mongolia
MR	Mauritania
MW	Malawi
MX	Mexico
NE	Niger
NL	Netherlands
NO	Norway
NZ	New Zealand
PL	Poland
PT	Portugal
RO	Romania
RU	Russian Federation
SD	Sudan
SE	Sweden
SG	Singapore
SI	Slovenia
SK	Slovakia
SN	Senegal
SZ	Swaziland
TD	Chad
TG	Togo
TJ	Tajikistan
TM	Turkmenistan
TR	Turkey
TT	Trinidad and Tobago
UA	Ukraine
UG	Uganda
US	United States of America
UZ	Uzbekistan
VN	Viet Nam
YU	Yugoslavia
ZW	Zimbabwe

METHOD AND SYSTEM FOR AUTOMATED DETECTION OF CLUSTERED MICROCALCIFICATIONS FROM DIGITAL MAMMOGRAMS

BACKGROUND OF THE INVENTION

1. Field of the Invention

This invention relates to a method and system for automated detection of clustered microcalcifications from digital images without reduction of radiologist sensitivity.

2. Discussion of Background

Mammography, along with physical examination, is the current procedure of choice for breast cancer screening. Screening mammography has been responsible for an estimated 30 to 35 percent reduction in breast cancer mortality rates. However, in 1996 approximately 185,700 new breast cancer cases were diagnosed and 44,300 women died from this disease. Women have about a 1 in 8 chance of being diagnosed with breast cancer, and 1 in 30 will die of this disease in her lifetime.

Although mammography is a well-studied and standardized methodology, for 10 to 30 percent of women diagnosed with breast cancer, their mammograms were interpreted as negative. Additionally, only 10 to 20 percent of patients referred for biopsy based on mammographic findings prove to have cancer. Further, estimates indicate the malignancies missed by radiologists are evident in two-thirds of the mammograms retrospectively. Missed detections may be attributed to several factors including: poor image quality, improper patient positioning, inaccurate interpretation, fibroglandular tissue obscuration, subtle nature of radiographic findings, eye fatigue, or oversight.

To increase sensitivity, a double reading has been suggested. However, the growing increase in the number of screening mammograms makes this option unlikely. Alternatively, a computer-aided diagnosis (CAD or CADx) system may act as a "second reader" to assist the radiologist in detecting and diagnosing lesions. Several investigators have attempted to analyze mammographic abnormalities with digital computers. However, the known studies are believed to have achieved rates of true-positive detections versus false-positive detections that

are undesirably low.

Microcalcifications represent an ideal target for automated detection because subtle microcalcifications are often the first and sometimes the only radiographic findings in early, curable breast cancers, yet individual microcalcifications in a suspicious cluster have a fairly limited range of radiographic appearances. Between 30 and 50 percent of breast carcinomas detected radiographically demonstrate microcalcifications on mammograms, and between 60 and 80 percent of breast carcinomas reveal microcalcifications upon microscopic examination. Any increase in the detection rate of microcalcifications by mammography will lead to further improvements in its efficacy in the detection of early breast cancer.

Although the promise of CAD systems is to increase the ability of physicians to diagnose cancer, the problem is that all CAD systems fail to detect some regions of interest that could be found by a human interpreter. However, human interpreters also miss regions of interest that are subsequently shown to be indicators of cancers. Missing a region that is associated with a cancer is termed a false negative error while associating a normal region with a cancer is termed a false positive error.

It is not yet clear how CAD system outputs are to be incorporated by practicing radiologists into their mammographic analyses. No existing CAD system can claim to find all of the suspicious regions detected by an average radiologist, and they tend to have unacceptably high false positive error rates. However, CAD systems are capable of finding some suspicious regions that may be missed by radiologists.

SUMMARY OF THE INVENTION

Accordingly, an object of this invention is to provide a method and system for automated detection of clustered microcalcifications from digital mammograms.

These and other objects are achieved according to the invention by providing a novel method and system for automated detection of clustered

microcalcifications from digital mammograms in which a digital mammogram is obtained, parameters necessary for cropping the digital mammogram image are optimized, the digital mammogram is cropped based on the optimized cropping parameters to select breast tissue for further analysis, parameters necessary for detecting clustered microcalcifications are optimized, and clustered microcalcifications in the cropped digital mammogram are detected based on the optimized clustered microcalcification detection parameters.

The detected clustered microcalcifications are then stored as a detections image, the detections image is processed for display, and a computer-aided detection image is produced for review by a radiologist.

The radiologist first reviews the original mammograms and reports a set of suspicious regions of interest, S1. A CAD system, or more particularly, the CAD system of the invention, operates on the original mammogram and reports a second set of suspicious detections or regions of interest, S2. The radiologist then examines the set S2, accepts or rejects members of S2 as suspicious, thus forming a third set of suspicious detections, S3, that is a subset of set S2. The radiologist then creates a fourth set of suspicious detections, S4, that is the union of sets S1 and S2, for subsequent diagnostic workups. CAD system outputs are thereby incorporated with the radiologist's mammographic analysis in a way that optimizes the overall sensitivity of detecting true positive regions of interest.

Other objects and advantages of the invention will be apparent from the following description, the accompanying drawings and the appended claims.

BRIEF DESCRIPTION OF THE DRAWINGS

Fig. 1 is a flow diagram illustrating the automated system for the detection of clustered microcalcifications in a digital mammogram;

Figs. 2 and 3 are flow diagrams illustrating the autocropping method and system of the invention;

Figs. 4-10 are flow diagrams illustrating in more detail the autocropping method and system of the invention;

Fig. 11 is a flow diagram illustrating in greater detail the clustered

microcalcification detector of the invention;

Fig. 12 is a schematic diagram illustrating a 3 × 3 cross-shaped median filter of the invention;

Fig. 13 is a three-dimensional plot of a Difference of Gaussians (DoG) filter kernel;

Fig. 14 is a cross-sectional view through the center of the DoG filter kernel of Fig. 13;

Fig. 15 is a flow diagram illustrating the global thresholding portion of the microcalcification detection system;

Fig. 16 is a flow diagram illustrating the dual local thresholding of the invention;

Fig. 17 is a flow diagram illustrating combining the results of global and dual-local thresholding;

Fig. 18 is a flow diagram illustrating the sloping local thresholding of the invention;

Fig. 19 is a flow diagram illustrating the clustering method of the invention;

Fig. 20 is a schematic diagram illustrating the clustering method of the invention;

Fig. 21 is a flow diagram illustrating the feature computation process of the invention;

Fig. 22 is a flow diagram illustrating a classifier having one discriminant function per class;

Fig. 23 is a schematic diagram illustrating a multi-layer perceptron neural network for a two-class classifier;

Fig. 24 is a histogram of testing results after detection and classification;

Fig. 25 is a flow diagram illustrating the parameter optimization method of the invention;

Fig. 26 is a plot of a free response receiver operating characteristic curve of the invention before classifying detections;

Fig. 27 is a plot of a free response receiver operating characteristic curve of the invention after classifying detections;

Fig. 28 is a plot of probability density functions showing the relationship between the probabilities of false negative and false positive detections;

Fig. 29 is a plot of probability density functions showing the relationship between the probabilities of true negative and true positive detections;

Fig. 30 is a Venn diagram showing the relationship between radiologist and CAD system detections;

Fig. 31 is a flow diagram illustrating a method for incorporating computer-aided diagnosis detections with those of a human interpreter for optimal sensitivity; and

Fig. 32 is a flow diagram illustrating an alternative embodiment of the invention that includes a density detector.

DETAILED DESCRIPTION OF THE PREFERRED EMBODIMENT

Referring now to the drawings, wherein like reference numerals designate identical or corresponding parts throughout the several views, and more particularly to Fig. 1 thereof, there is shown a flow diagram illustrating a sequence of steps performed in order to detect the locations of clusters of microcalcifications within a digital mammogram.

In a first step 100, a digital mammogram is obtained using hardware such as digital mammography systems, or by digitizing mammography films using laser or charge-coupled device (CCD) digitizers. In an optimized cropping step 200, a rectangular analysis region containing breast tissue is segmented from the digital mammogram image and a binary mask corresponding to the breast tissue is created for use in later processing steps to decrease the time required for processing the mammogram image. The binary mask is also used to limit detections to areas of the image containing breast tissue.

Clustered microcalcifications are detected in a clustered microcalcification detection step 300. After first filtering the cropped image with a median filter to reduce noise, the image is filtered using an optimized difference of

Gaussians (DoG) filter to enhance the microcalcifications. The DoG-filtered image is then subjected to optimized threshold tests to detect potential microcalcifications. The detected microcalcifications are shrunk to single-pixel representations and detections outside of the breast area are removed. The remaining microcalcifications are grouped into clusters. Features are then computed for the clusters. Detected clusters are classified as either suspicious or non-suspicious in a classification step 400.

The parameters used by the autocropping, clustered microcalcification detection, and classification steps 200, 300, 400 are optimized in a parameter-optimizing step 500. The parameters are optimized by parameter-optimizing means that uses a genetic algorithm (GA) so as to maximize the true-positive detection rate while minimizing the false-positive detection rate. Of course, other optimization schemes may be used as well.

The detected clustered microcalcifications are stored in a list of image coordinates. The detection results are processed in a processing step 600 by simply adding an offset to each of the microcalcification coordinates to account for translation of the coordinates incurred as a result of the cropping procedure. Detected clustered microcalcifications are indicated on the digital mammogram by means of rectangles drawn around the clustered microcalcifications in a display step 700. Other indicators may be used such as, for example, arrows pointing to suspected microcalcifications, or ellipses around suspected microcalcifications.

ACQUIRING A DIGITAL REPRESENTATION OF A MAMMOGRAM

One method of obtaining digital mammograms comprises digitizing radiologic films by means of a laser or charge-coupled device (CCD) scanner. Digital images obtained in this manner typically have a sample spacing of about 100 μm per pixel, with a gray-level resolution of 10 to 12 bits per pixel. In one embodiment of the present invention, radiologic films are scanned using a Model CX812T digitizer manufactured by Radiographic Digital Imaging of Compton, California, to produce digital images having 50 μm spacing per pixel and 12 bits of gray-level resolution per pixel. Another possible input source for digital images is a

digital mammography unit from Trex Medical Corporation of Danbury, Connecticut, which has a spatial resolution of about 45 μm per pixel and a gray-level resolution of 14 bits per pixel.

The digital images are stored as digital representations of the original mammogram images on computer-readable storage media. In a preferred embodiment, the digital representations or images are stored on a 2 GB hard drive of a general-purpose computer such as a PC having dual Pentium II ® microprocessors running at 200 MHZ, 512 MB of RAM memory, a ViewSonic PT813 ® monitor, a pointing device, and a Lexmark Optra S1625 ® printer. The system operates within a Windows NT ® operating system.

AUTOCROPPING

As may be seen in Figs. 2 and 3, a digital mammogram image 190 is first cropped to segment an analysis region 296 from the image and produce a binary mask 298 corresponding to breast tissue in the analysis region. Preferably, the cropping is performed automatically, although it could be cropped manually. The image is cropped as a preliminary step because the breast tissue does not cover the whole radiographic film. Focusing the processing of the image on only that portion of the image which breast tissue reduces the time required to process the image. Also, other items appearing on the film, such as labels and patient information, are excluded from consideration, and false-positive indications lying outside of the breast tissue area are eliminated.

Referring to Figs. 4 through 10, the autocropping process will be described in detail. The image is first subsampled from 50 μm to 400 μm to reduce the amount of data to be processed in step 202. Of course, the image may be downsampled to other resolutions as desired. Not all of the original image data is needed to reliably segment the breast tissue from the remainder of the image. Subsampling every eighth pixel in both the horizontal and vertical directions reduces the amount of data by 64 times. For purposes of segmenting the breast tissue from the rest of the image, the consequent loss of resolution is immaterial.

A white border twenty pixels in width is added around all sides of the

subsampled image in step 204. White corresponds to the maximum pixel value possible given the number of bits used to represent each pixel. For images having 12 bits of gray-scale resolution, the maximum gray-scale value is 4095. The bordered image is then thresholded in step 206 with a relatively high threshold value such that most of the breast tissue is guaranteed to be less than the threshold to produce a binary image. In one embodiment of the invention, the threshold is set equal to a predetermined percentage of the gray-scale value of a pixel near the top middle portion of the image. The thresholded image is then inverted, that is, ones become zeroes and zeroes become ones, in step 208. The inverted image is then dilated in step 210. Dilation is a morphological operation in which each pixel in a binary image is turned on, that is, set to a value of one, if any of its neighboring pixels are on. If the pixel is already on, it is left on.

In step 212 the dilated image is cropped to the size of the largest blob. Blobs are contiguous groups of pixels having the value one. This step 212 removes bright borders from the subsampled mammogram representation while ensuring that none of the breast area is reduced. Other techniques that threshold to find the border have a very difficult time dealing with bright areas in the breast adjacent to the border such as, for example, when breast implants are visible in the image. Pixels from the original image, resulting from step 202, corresponding to the locations of the pixels in the cropped blob, are selected for subsequent processing. Note that this is a simple subset of pixels from the input image.

The image from step 212 is histogram equalized in step 214. The average brightness of the image will vary widely from mammogram to mammogram. Moreover, different digitizers having different optical density characteristics are an additional source of variability in brightness levels in the digital representation of the mammogram. The breast mask that is the output of the autocropper is mainly defined by means of a region-growing algorithm that requires a single contrast setting to work properly. However, it has been determined experimentally that a single contrast setting will not work for a wide range of image inputs. Therefore, each image is mapped into a normalized image space using an automatic histogram enhancement process, after which a single contrast setting works well.

First, a histogram of the image is obtained. Typically, most of the data in the breast area will be in the lower histogram bins (corresponding to gray-scale values of about 0 - 1000), with borders and labels being in the higher bins (corresponding to gray-scale values of about 4000 - 4095) for 12-bit data. The upper and lower bin values that contain the typical breast data are determined. The lower bin value is the first highest peak encountered when going from the lowest gray-scale value toward the highest gray-scale value. The upper bin is the last zero-value bin encountered when going from the highest gray-scale level toward the lowest gray-scale value. Then the data are reduced to an eight-bit representation and linearly stretched over the range of the data type. For example, values in the lower bins are set to zero. Values of data in the upper bins are set to 255. The rest of the data are then linearly mapped between the lower and upper bins.

After the image has been histogram equalized, the equalized image may be considered to be a matrix. The image matrix is divided into left and right halves, of equal size if possible, and the brighter side is selected in a step 216. The sums of all the pixels in the left and right halves are computed. The sum values are then compared and the side having the greater sum is the brighter side.

Prior to region growing the brighter side, algorithm variables are initialized in step 218. The size of the region-grown mask is preliminarily checked in step 220. If it is large enough, then the mask is acceptable. Otherwise, processing continues to find the mask. The side of the image to be region grown is selected in step 222. In step 224 this region is searched to find its maximum gray-scale value. This maximum value is used to find a pixel to start a region-growing algorithm. Region growing is the process of grouping connected pixels sharing some like characteristic. The choice of characteristic influences the resultant region. The input to a region growing function is a gray-scale image and a starting point to begin growing. The output is a binary image with ones indicating pixels within the grown region, *i.e.*, blobs. Region growing will create a single blob, but that blob may have within it internal holes, that is, pixels that are off. To grow a blob, each of the four nearest neighbors of a pixel of interest are looked at. The contrast ratio is computed for each nearest neighbor pixel. If the contrast ratio is less than a contrast ratio

threshold, then the neighbor pixel is set to a one in a binary mask image. Otherwise, the neighbor pixel is set to zero. The region growing algorithm spirals outwardly from the starting or seed pixel, progressively looking at nearest neighbor pixels until done. To those skilled in the art, it is clear that other region growing algorithms may also be applied.

In step 226, region growing begins with the pixel identified from the previous step 224 to produce a binary mask. The size of the mask resulting from step 226 is computed in step 228 and checked in step 230. There may be three points of failure for this approach. First, the brightest point in the search region may be an artifact outside the breast. Therefore, if the resulting mask is not large enough (50 pixels), then the search region is moved closer to the side of the image and searched again. This is repeated three times, each time lowering the contrast value threshold. This corresponds to the path taken through steps 232 and 234. Second, the side selection approach may be in error. Therefore, if a valid breast mask is not found in the first side searched, then the other side of the breast is searched. This corresponds to the path taken through steps 236 and 238. Third, if a valid breast mask is not found on either side, then the whole breast is thresholded and the largest object is taken to be the breast mask in step 240.

Since a constant contrast value is used in the region-growing algorithm, some masks will be too large. Typically, there will be "tails" along the edge of the digitized mammogram image where extra light leaked in while the original mammogram film was being digitized. The tails are reduced by applying a series of erodes and then a series of dilates to the image. Erosion is a morphological operation in which each pixel in a binary image is turned off unless all of its neighbors are on. If the pixel is already off, it is left off. But first, the holes in the mask must be filled in or the multiple erodes may break the mask into disjoint sections. Thus, holes in the mask are closed in step 242 by means of a majority operation. The majority operation is a morphological operation in which each pixel in a binary image is turned on if a majority of its neighboring pixels are on. If the pixel is already on, it is left on.

However, another problem is that some smaller breast masks can not

undergo as many erodes as can larger breast masks. Therefore, as a fail-safe measure, the sum of the breast mask is taken before and after the erodes and dilates. If the size is reduced too much (*i.e.*, by more than 50%), the original mask before the morphological operators is used. Thus, a duplicate copy of the mask is made in step 244 before the mask is eroded and dilated in steps 246 and 248, respectively. The size of the resultant mask is then computed in step 250 and compared with the size of the mask from step 242 in step 252. If the new size is less than half the old size, then the duplicate mask, from step 244, is selected in step 254 for subsequent processing. Otherwise, the resultant mask from step 248 is used.

The original image (from step 202) is then cropped to the size of the breast mask just found (either from step 242 or step 248) in step 256. In case the resulting mask is too small for subsequent processing, a crop adjustment is always made in step 258. The adjustment comes in the form of increasing the size of the breast mask bounding box by including additional pixels from the original image in the cropped image.

The cropped image is then automatically histogram enhanced in step 260 as previously described above in connection with step 214. This enhanced image is passed through a loose region growing step 262 to produce a generous mask. This means that the image is subjected to a lower threshold to yield more "on" pixels. This mask is then subjected to hole-closing, eroding, and dilating in steps 264, 266, and 268, respectively, as above, but to a lesser degree.

The same steps described above are repeated one final time in steps 270 through 276, but the crop adjustments are less and the contrast value is increased for a tight region growing step 276. This tight region growing step 276 can afford the higher contrast value since it will be region growing in just the cropped image. This results in a parsimonious estimate of breast tissue. The resulting mask is segmented to find the largest object in step 278 and its bounding box shrunk to just enclose the object in step 280. There may still be some holes in the breast mask. Therefore, after crop adjustments in step 282, the mask is inverted in step 284 and the largest object is found in step 286. This largest object is extracted and then inverted in step 288 to obtain the penultimate mask.

The final mask is obtained by closing holes in the penultimate mask with multiple majority operations and dilations in step 290. The image is then cropped to the size of the resulting mask and the autocropping is complete. An important result from the autocropper is the offset of the cropped image. This is the pixel location in the original image that corresponds to the pixel in the upper left pixel of the cropped image. Keeping track of all the cropping and crop adjustments determines this offset value.

The output of the autocropping process is a rectangular array of pixels representing a binary mask wherein the pixels corresponding to breast tissue are assigned a value of one while the remainder of the pixels are assigned a value of zero. Put another way, the binary mask is a silhouette of the breast made up of ones while the background is made up of zeroes.

Parameters of the autocropper may be optimized to obtain better breast masks. The procedure is described below in the optimization section.

DETECTION OF CLUSTERED MICROCALCIFICATIONS

Turning now to Fig. 11, there is seen therein a flow diagram illustrating in greater detail the clustered microcalcification detection system 300 of the invention.

That portion of the digital representation of the mammogram corresponding to the analysis region 296, designated a cropped sub-image 302, produced in the cropping step 200, is first processed to reduce noise in a noise reduction step 310 to reduce digitization noise that contributes to false detections of microcalcifications. The noise-reduced image is then filtered using an optimized target-size-dependent difference of Gaussians (DoG) spatial kernel in step 320 to enhance differences between targets and background, thus creating global and local maxima in the filtered image. The optimized DoG-filtered image is then thresholded in step 340 to segment maxima that represent potential detections of microcalcifications.

The detected maxima are converted to single-pixel coordinate representations in a conversion step 350. The coordinate representations of the

detected maxima are compared with the binary mask of the analysis area in a first false-positive removal step 360 to remove false detections outside the breast mask area. The remaining coordinate representations in the analysis area are clustered in a clustering step 370. Features are computed for the remaining clusters in a feature computation step 380 and used to remove non-suspicious detections in a classifying step 400 (Fig. 1). The remaining detections are outputted as detected clustered microcalcifications in an outputting step 600 in the form of cluster coordinates.

Turning now to a more detailed discussion of the steps in the clustered microcalcification detection process, the digital mammogram image is first filtered to reduce noise in the image. Although the main limitation in image quality should be the granularity of the film emulsion, noise is introduced from the process of digitization. This noise may later be detected as a pseudocalcification. In this system, a cross-shaped median filter is used because it is well known to be extremely effective at removing single-pixel noise. The median filter is a non-linear spatial filter that replaces each pixel value with the median of the pixel values within a kernel of chosen size and shape centered at a pixel of interest. Referring to Fig. 12, it may be seen that the cross shape is formed by the set of pixels which include the center pixel and its four nearest neighbors. The cross shape preserves lines and corners better than typical block-shaped median filters and limits the possible substitution to the four nearest neighbors, thereby reducing the potential for edge displacement.

After noise has been reduced, the image is filtered with an optimized DoG kernel to enhance microcalcifications. Filtering is accomplished by convolving the noise-reduced image with the DoG kernel. In an alternative embodiment, filtering is accomplished by first obtaining the fast Fourier transforms (FFTs) of the noise-reduced image and the DoG kernel, then multiplying the FFTs together, and taking the inverse FFT of the result.

The DoG kernel was chosen because neurophysiological experiments provide evidence that the human visual pathway includes a set of "channels" that are spatial frequency selective. Essentially, at each point in the visual field, there are size-tuned filters or masks analyzing an image. The operation of these spatial

receptive fields can be approximated closely by a DoG.

The 2-D Gaussian mask is given as:

$$G(x,y) = ce^{\frac{-(x^2+y^2)}{2\sigma^2}} \quad (1)$$

where c normalizes the sum of mask elements to unity, x and y are horizontal and vertical indices, and σ is the standard deviation. Using Equation 1, the difference of two Gaussians with different σ yields:

$$DoG(x,y) = c_1 e^{\frac{-(x^2+y^2)}{2\sigma_1^2}} - c_2 e^{\frac{-(x^2+y^2)}{2\sigma_2^2}} \quad (2)$$

It has been shown that when $\sigma_2 = 1.6\sigma_1$, then the DoG filter's response closely matches the response of human spatial receptive filters. Therefore, with motivation from human physiology, let the ratio of the DoG standard deviation constants be 1:1.6. Then, for a target of size (average width) t pixels, use $\sigma_2 = t/2$ and, from the rule of thumb, $\sigma_1 = \sigma_2/1.6$.

Since microcalcifications typically range from 100 to 300 μm in diameter, potential target sizes for the 50 μm digitized mammograms correspond to 2 to 6 pixels. It has been found that a DoG kernel constructed using an optimization technique for selecting the target size parameter, such as the GA detailed below, has an optimized target size of $t = 6.01$ pixels. The targetsize t will vary depending on such factors as the resolution and scale of the image to be processed. The impulse response of a DoG filter having t = 6.01 pixels and $\sigma_2 = 1.6\sigma_1$ is shown in Figs. 13 and 14.

Once the noised-reduced cropped image has been DoG filtered to enhance differences between targets and background, the DoG-filtered subimage contains differences in gray levels between potential microcalcifications and background. Although microcalcifications tend to be among the brightest objects in DoG-filtered subimages, they may exist within regions of high average gray levels and thus prove difficult to reliably segment. The thresholding process used in one

embodiment of the invention that generally addresses these concerns involves pair-wise pixel "ANDing" of the results of global histogram and locally adaptive thresholding. However, the preferred embodiment of the invention uses sloping local thresholding.

Since targets tend to exist within an image's higher gray levels, then the global threshold may be approximated by finding the level which segments a preselected percentage of the corresponding higher pixel levels in the image histogram. An embodiment of a global thresholding method is illustrated in Fig. 15. Locally adaptive thresholding may be implemented by varying the high and low thresholds based on the local pixel value mean and standard deviation. An embodiment of a dual-local thresholding method is illustrated in Fig. 16.

After computing the image histogram, $p(r_k)$, the gray level threshold, g, used to segment a preselected upper fraction, f, of the histogram, is found using:

$$f = 1 - \sum_{k=0}^{g} p(r_k) \qquad (3)$$

where r_k is the k^{th} gray level, $0 \le g \le g_{max}$, and g_{max} is the maximum gray level in the image.

The locally adaptive thresholds, t_{lo} and t_{hi}, are found using

$$t_{lo} = k_{lo}\sigma_{NN}(x,y) + \mu_{NN}(x,y) \qquad (4)$$

and

$$t_{hi} = k_{hi}\sigma_{NN}(x,y) + \mu_{NN}(x,y) \qquad (5)$$

where k_{lo} and k_{hi} are used to preselect the multiple of $\sigma_{NN}(x,y)$, the local standard deviation of gray-level intensities, and $\mu_{NN}(x,y)$ is the local gray-level mean of the $N \times N$ neighborhood centered on the pixel at (x,y) of the DoG-filtered image. Other neighborhood shapes, such as rectangular, circular, and ellipsoidal, may also be used. Pixels whose brightness or gray-level value falls within the threshold interval, that is, $t_{lo} <$ brightness $< t_{hi}$, are set equal to one. Optimization of f, k_{lo}, k_{hi}, and N is

discussed below in connection with the parameter-optimizing process. The results of the global thresholding process may be combined with the results of the local thresholding step by logically ANDing them as shown in Fig. 17. Alternatively, either thresholding method may be used alone.

The preferred thresholding means are illustrated in Fig. 18 wherein it may be seen that an N × N window is centered at a pixel x,y in the input image p(x,y). The mean, $\mu(x,y)$, and standard deviation, $\sigma(x,y)$, of the digital mammogram image pixels under the window are computed. A local threshold value, T(x,y), is computed as:

$$T(x,y) = A + B\mu(x,y) + C\sigma(x,y) \quad (6)$$

where values for N, A, B, and C are computed during a parameter optimization stage, discussed below. Values for T(x,y) are computed for every x,y location in the image.

The digital mammogram has also been DoG filtered, producing an image d(x,y). Each pixel of the DoG-filtered image d(x,y) is compared to the threshold value T(x,y). Pixels in the locally thresholded image $l_s(x,y)$ are set to one where values of the DoG-filtered image are greater than the threshold, and set to zero elsewhere.

The advantage of this novel local sloping thresholding method over prior art thresholding methods is that the threshold is computed from the pixels in a pre-DoG-filtered image rather than from a post-DoG-filtered image. This eliminates the need for background trend correction. In conventional local thresholding, the threshold is computed as:

$$T(x,y) = B\mu(x,y) + C\sigma(x,y) \quad (7)$$

from the mean and standard deviation of the DoG-filtered image. The problem of using a local threshold computed from the DoG-filtered image is that DoG-filtered images typically have mean values close to zero and standard deviations significantly affected by the presence of targets.

Local thresholds computed from the statistics of the DoG-filtered image suffer from the following adverse effects. First, since the mean value is close

to zero, a degree of freedom is lost in the computation of the threshold, which becomes essentially a function of the standard deviation. Second, the absolute brightness of the input image is lost. To keep many spurious detections from occurring, it is desirable to have high thresholds in bright regions. However, the information about the local mean of the input image is not available in the DoG-filtered image. Finally, the standard deviations of DoG-filtered images are increased by detections of targets. This is so because when local bright spots of proper size exist in the original image, large gray-scale values result in the DoG-filtered image. Thus, the presence of targets in a region increases the local standard deviation thereby raising the threshold of that region. The higher threshold reduces the probability of passing a bright spot to subsequent processing stages.

The novel local thresholding method just described solves the above problems by computing thresholds from the input image, which are then applied to the DoG-filtered image. Additionally, the threshold computed here includes an offset term A, which is independent of the local image mean.

After thresholding, detections are converted to single-pixel representations by computing the centroid or center of gravity of groups of contiguous pixels found by the thresholding process. Detections are thus represented as single pixels having a value of logical one while the remaining pixels have a value of logical zero.

False-positive detections outside of the breast area are removed by logically ANDing the binary mask from the autocropper with the single-pixel representations of the detections.

Calcifications associated with malignancies usually occur in clusters and can be extensive. The cluster detection module identifies clusters based on a clustering algorithm as depicted in Fig. 19. Specifically, a suspicious cluster is declared when at least μCs_{min} or more detected signals are separated by less than a nearest neighbor distance, d_{nn}. Optimization of μCs_{min} and d_{nn} is discussed below in connection with the parameter optimizing process. Figure 20 illustrates the clustering process for the case wherein $\mu Cs_{min} = 5$ and $d_{nn} = 4$.

Additional false-positive clustered microcalcifications are removed by

means of a classifier, detailed below. Features are extracted for each of the potential clustered microcalcifications as shown in Fig. 21. The eight features computed for each of the potential clustered microcalcifications in a preferred embodiment are:

1. The larger eigenvalue (λ_1) of the covariance matrix of the points in a cluster;

2. The smaller eigenvalue (λ_2) of the covariance matrix of the points in a cluster;

3. The ratio of the smaller eigenvalue of the covariance matrix to the larger eigenvalue of the covariance matrix of the points in a cluster. Equivalent to the ratio of the minor axis to the major axis of an ellipse fitted to cover the points in a cluster;

4. Linear density calculated as the number of detected microcalcifications divided by the maximum interpoint distance;

5. Standard deviation of the distances between points in a cluster;

6. Mean minus median of the distances between points in a cluster;

7. Range of points in cluster calculated as maximum interpoint distance minus the minimum interpoint distance; and

8. Density of a cluster calculated as the number of detections divided by the area of a box just large enough to enclose the detections.

Of course, other features could be computed for the potential microcalcification clusters, and the invention is not limited to the number or types of features enumerated herein.

CLASSIFYING DETECTIONS

The cluster features are provided as inputs to the classifier, which classifies each potential clustered microcalcification as either suspicious or not suspicious. In practice, the clustered microcalcification detector is only able to locate regions of interest in the digital representation of the original mammogram that may be associated with cancer. In any detector, there is a tradeoff between locating as many potentially suspicious regions as possible versus reducing the number of normal regions falsely detected as being potentially suspicious. CAD

systems are designed to provide the largest detection rates possible at the expense of detecting potentially significant numbers of regions that are actually normal. Many of these unwanted detections are removed from consideration by applying pattern recognition techniques.

Pattern recognition is the process of making decisions based on measurements. In this system, regions of interest or detections are located by a detector, and then accepted or rejected for display. The first step in the process is to characterize the detected regions. Toward this end, multiple measurements are computed from each of the detected regions. Each measurement is referred to as a feature. A collection of measurements for a detected region is referred to as a feature vector, wherein each element of the vector represents a feature value. The feature vector is input to a discriminant function.

Referring to Fig. 22, there may be seen therein a classifier having a feature vector x applied to a set of discriminant functions $g(x)$. The classifier shown in Fig. 22 is designed with one discriminant function per class. A discriminant function computes a single value as a function of an input feature vector. Discriminant functions may be learned from training data and implemented in a variety of functional forms. The output of a discriminant function is referred to as a test statistic. Classification is selecting a class according to the discriminant function with the greatest output value. The test statistic is compared to a threshold value. For values of the test statistic above the threshold, the region or detection associated with the feature vector is retained and displayed as potentially suspicious. When the test statistic is below the threshold, the region is not displayed.

Many methods are available for designing discriminant functions. One approach considered for this invention is a class of artificial neural networks. Artificial neural networks require training, whereby the discriminant function is formed with the assistance of labeled training data.

In a preferred embodiment, the classification process is implemented by means of a multi-layer perceptron (MLP) neural network (NN). Of course, other classifier means could be used such as, for example, a statistical quadratic classifier. Only potential clustered microcalcifications classified as suspicious are retained for

eventual designation for a radiologist. Alternatively, it may be desirable to iteratively loop between MLP NN analysis of the individual microcalcification detections and the microcalcification clusters.

Referring to Fig. 23, a schematic diagram of an MLP NN may be seen therein. The MLP NN includes a first layer of J hidden layer nodes or perceptrons 410, and one output node or perceptron 420 for each class. The preferred embodiment of the invention uses two output nodes, one each for the class of suspicious detections and the class of non-suspicious detections. Of course, more or fewer classes could be used for classifying clusters of microcalcifications. Each computed feature x_i is first multiplied by a weight $w_{i,j}$, where i is an index representing the i^{th} feature vector element, and j is an index representing the j^{th} first layer node. The output y_j of each first layer perceptron 410 is a nonlinear function of the weighted inputs and is given by:

$$y_j = f\left(\sum_{i=1}^{d} (w_{i,j} \times x_i)\right) \tag{8}$$

where d represents the total number of features x_i and f(•) is typically a saturating nonlinearity. In this embodiment, f(•) = tanh(•). The first layer or hidden layer node outputs y_j are then multiplied by a second layer of weights $u_{j,k}$ and applied to the output layer nodes 420. The output of an output layer node 420 is a nonlinear function of the weighted inputs and is given by:

$$z_k(y) = f\left(\sum_{j=1}^{J} (u_{j,k} \times y_j)\right) \tag{9}$$

where k is an index representing the k^{th} output node.

The hyperbolic tangent function is used in a preferred embodiment of the system because it allows the MLP NN to be trained relatively faster as compared to other functions. However, functions other than the hyperbolic tangent may be used to provide the outputs from the perceptrons. For example, linear functions may be used, as well as smoothly varying nonlinear functions, such as the sigmoid

function.

The weight values are obtained by training the network. Training consists of repeatedly presenting feature vectors of known class membership as inputs to the network. Weight values are adjusted with a back propagation algorithm to reduce the mean squared error between actual and desired network outputs. Desired outputs of z_1 and z_2 for a suspicious input are +1 and -1, respectively. Desired outputs of z_1 and z_2 for non-suspicious inputs are -1 and +1, respectively. Other error metrics and output values may also be used.

In this embodiment of the system, the MLP NN is implemented by means of software running on a general-purpose computer. Alternatively, the MLP NN could also be implemented in a hardware configuration by means readily apparent to those with ordinary skill in the art.

After training, each detected clustered microcalcification is classified as either suspicious or not suspicious by means forming the difference $z_1 - z_2$, then comparing the difference to a threshold, θ. For values of $z_1 - z_2$ greater than or equal to the threshold θ, *i.e.*, $z_1 - z_2 \geq \theta$, the classifier returns a value of +1 for suspicious clustered microcalcifications, and for values of $z_1 - z_2 < \theta$, the classifier returns a value of -1 for non-suspicious clustered microcalcifications.

In order to arrive at optimum values for the respective weights, and the number of first layer nodes, the MLP NN was trained with a training set of feature vectors derived from a database of 978 mammogram images.

To develop and test the CAD system of the invention, truth data was first generated. Truth data provides a categorization of the tissue in the digital images as a function of position. Truth data was generated by certified radiologists marking truth boxes over image regions associated with cancer. In addition to the mammogram images, the radiologists also had access to patient histories and pathology reports.

The radiologists identified 57 regions of interest, containing biopsy-confirmed cancers associated with clustered microcalcifications, by means of truth boxes. All 978 images were then processed by the microcalcification detector of the invention to produce a plurality of feature vectors, a subset of which were associated

with the 57 truth boxes. Half of the subset feature vectors were randomly chosen, along with about three times as many feature vectors not associated with clustered microcalcifications, to comprise the training set of feature vectors. The MLP NN, having a predetermined number of hidden nodes, was then trained using the training set. The remaining feature vectors were used as a test database to evaluate the performance of the MLP NN after training. Training of the MLP NN was carried out by means of the Levenberg-Marquardt back propagation algorithm.

Alternatively, the MLP NN can be trained with other learning algorithms and may have nonlinearities other than the hyperbolic tangent in either or both layers. In an alternative embodiment with sigmoidal output nodes, the Bayes optimal solution of the problem of classifying clustered microcalcification detections as either suspicious or non-suspicious may be obtained.

In one run of the preferred embodiment during testing, before application of the MLP NN classifier to eliminate false-positive clustered microcalcifications, the detection procedure found about 93% of the true-positive clustered microcalcifications in both the training and test databases while indicating about 10 false-positive clustered microcalcifications per image. It was found that after an MLP NN classifier having 25 first layer nodes was used with the respective optimum weights found during training, 93% of the true-positive detections were retained while 57% of the false-positive detections were successfully removed. Referring to Fig. 24, there may be seen a histogram of the results of testing on the testing database after classification by the MLP NN. Of course, the MLP NN of the invention may be operated with more or fewer first layer nodes as desired.

DISPLAYING DETECTIONS

After the locations of clustered microcalcifications have been determined, they are indicated on the original digitized mammogram image, or a copy of the original image, by drawing rectangular boxes around microcalcifications. Other means for indicating the locations of microcalcifications may be used, such as, for example, placing arrows in the image pointing at detections or drawing ellipses around the detections.

The locations of clustered microcalcifications are passed to the display detections procedure as a list of row and column coordinates of the upper left and lower right pixels bounding each of the clusters. The minimum row and column coordinates and maximum row and column coordinates are computed for each cluster. Bounding boxes defined by the minimum and maximum row and column coordinates are added to the original digitized image, by means well known in the art. The resulting image is then stored as a computer-readable file, displayed on a monitor, or printed as a hard-copy image, as desired.

In one embodiment of the system, the resulting image is saved to a hard disk on a general-purpose computer having dual Pentium II ® processors and running a Windows NT ® operating system. The resulting image may be viewed on a VGA or SVGA monitor, such as a ViewSonic PT813 ® monitor, or printed as a hard-copy gray-scale image using a laser printer, such as a Lexmark Optra S1625 ®. Of course, other hardware elements may be used by those with ordinary skill in the art.

OPTIMIZING THE PARAMETERS

Genetic algorithms (GAs) have been successfully applied to many diverse and difficult optimization problems. A preferred embodiment of this invention uses an implementation of a GA developed by Houck, et al. ("A Genetic Algorithm for Function Optimization," Tech. Rep., NCSU-IE TR 95-09, 1995), which is incorporated by reference herein, to find promising parameter settings. The parameter optimization process of the invention is shown in Fig. 25. This is a novel application of optimization techniques as compared to current computer-aided diagnosis systems require hand tuning by experiment.

GAs search the solution space to maximize a fitness (objective) function by use of simulated evolutionary operators such as mutation and sexual recombination. In this embodiment, the fitness function to be maximized reflects the goals of maximizing the number of true-positive detections while minimizing the number of false-positive detections. GA use requires determination of several issues: objective function design, parameter set representation, population initialization,

choice of selection function, choice of genetic operators (reproduction mechanisms) for simulated evolution, and identification of termination criteria.

The design of the objective function is a key factor in the performance of any optimization algorithm. The function optimization problem for detecting clustered microcalcifications may be described as follows: given some finite domain, D, a particular set of cluster detection parameters , $x = \{t, f, k_{lo}, k_{hi}, N, \mu Cs_{min}, d_{nn}\}$ where $x \in D$, and an objective function $f_{obj} : D \rightarrow \Re$, where $\Re$ denotes the set of real numbers, find the x in D that maximizes or minimizes f_{obj}. When sloping local thresholding is used in the cluster detector, the parameters N, A, B, and C are optimized. Radiologic imaging systems may be optimized to maximize the TP rate subject to the constraint of minimizing the FP rate. This objective may be recast into the functional form shown in the following equation:

$$f_{obj}(x) = \begin{cases} -FP(x) & , TP(x) \geq TP_{min} \\ FP_{penalty} & , \text{otherwise} \end{cases} \qquad (10)$$

where maximization is the goal. For a particular set of cluster detection parameters, if the minimum acceptable TP rate, TP_{min}, is exceeded, the objective function returns the negative of the FP rate. Otherwise, if the TP rate falls below TP_{min}, the objective function returns a constant value, $FP_{penalty} = -10$. Other objective functions may also be used.

Since a real-valued GA is an order of magnitude more efficient in CPU time than the binary GA, and provides higher precision with more consistent results across replications, this embodiment of the invention uses a floating-point representation of the GA.

This embodiment also seeds the initial population with some members known beforehand to be in an interesting part of the search space so as to iteratively improve existing solutions. Also, the number of members is limited to twenty so as to reduce the computational cost of evaluating objective functions.

In one embodiment of the invention, normalized geometric ranking is used, as discussed in greater detail in Houck, et al., *supra*, for the probabilistic

selection process used to identify candidates for reproduction. Ranking is less prone to premature convergence caused by individuals that are far above average. The basic idea of ranking is to select solutions for the mating pool based on the relative fitness between solutions. This embodiment also uses the default genetic operation schemes of arithmetic crossover and nonuniform mutation included in Houck, et al.'s GA.

This embodiment continues to search for solutions until the objective function converges. Alternatively, the search could be terminated after a predetermined number of generations. Although termination due to loss of population diversity and/or lack of improvement is efficient when crossover is the primary source of variation in a population, homogeneous populations can be succeeded with better (higher) fitness when using mutation. Crossover refers to generating new members of a population by combining elements from several of the most fit members. This corresponds to keeping solutions in the best part of the search space. Mutation refers to randomly altering elements from the most fit members. This allows the algorithm to exit an area of the search space that may be just a local maximum. Since restarting populations that may have converged proves useful, several iterations of the GA are run until a consistent lack of increase in average fitness is recognized.

Once potentially optimum solutions are found by using the GA, the most fit GA solution may be further optimized by local searches. An alternative embodiment of the invention uses the simplex method to further refine the optimized GA solution.

The autocropping system may also benefit from optimization of its parameters including contrast value, number of erodes, and number of dilates. The method for optimizing the autocropper includes the steps of generating breast masks by hand for some training data, selecting an initial population, and producing breast masks for training data. The method further includes the steps of measuring the percent of overlap of the hand-generated and automatically-generated masks as well as the fraction of autocropped breast tissue outside the hand-generated masks. The method further comprises selecting winning members, generating new members, and

iterating in a like manner as described above until a predetermined objective function converges.

In Figures 26 and 27, there may be seen therein free response receiver operating characteristic curves for the system of the invention for the outputs of the optimized microcalcification detector and the classifier, respectively. Figure 26 represents the performance of the optimized detector before classifying detections, while Fig. 27 represents the performance of the system after classifying detections.

Although the GA has been described above in connection with the parameter optimization portion of the preferred embodiment, other optimization techniques are suitable such as, for example, response surface methodology. Of course, processing systems other than those described herein may be optimized by the methods disclosed herein, including the GA.

INCORPORATING CAD SYSTEM OUTPUTS FOR OPTIMAL SENSITIVITY

Performance metrics for detection of suspicious regions associated with cancer are often reported in terms of sensitivity and specificity. Sensitivity measures how well a system finds suspicious regions and is defined as the percentage of suspicious regions detected from the total number of suspicious regions in the cases reviewed. Sensitivity is defined as:

$$\text{Sensitivity} = \frac{TP}{TP + FN} \tag{11}$$

where TP is the number of regions reported as suspicious by a CAD system that are associated with cancers, and FN is the number of regions that are known to be cancerous that are not reported as suspicious. Specificity measures how well the system reports normal regions as normal. Specificity is defined as:

$$\text{Specificity} = \frac{TN}{FP + TN} \tag{12}$$

where TN represents regions correctly identified as not suspicious and FP represents regions reported as suspicious that are not cancerous.

Current CAD systems increase specificity by reducing FP. However, FP and TP are coupled quantities. That is, a reduction of FP leads to a reduction of TP. This implies that some of the suspicious regions that could have been detected are missed when the objective is to maintain high specificity.

Figures 28 and 29 illustrate relationships between the quantities TP, FP, TN, and FN. A measurement from a screening mammography image is represented by test statistic, x. The probability density function of x is represented by $p(x)$ and the decision threshold is represented by θ. If x is greater than θ, a suspicious region is reported. Areas under the probability density functions represent probabilities of events. From Fig. 28 observe that increasing the threshold reduces the probability of FP decisions. However, observe from Fig. 29 that increasing the threshold simultaneously reduces the probability of TP decisions.

Another metric that exists for CAD systems is positive predictive value (PPV), which is defined as the probability that cancer actually exists when a region of interest is labeled as suspicious. PPV can be calculated from the following equation:

$$PPV = \frac{TP}{TP + FP} \tag{13}$$

Note that increasing TP or reducing FP increases PPV.

Radiologists and computers find different suspicious regions. Figure 30 is a Venn diagram depicting a possible distribution of suspicious regions for man and machine detections. Some suspicious regions are found solely by a human interpreter or radiologist, some solely by a CAD system, some are found by both, and some are not found by either.

Referring to Fig. 31, there may be seen a preferred method for incorporating the outputs of a CAD system, and more particularly for the CAD system of the invention, with the observations of a human interpreter of a screening mammography image 10 for optimal sensitivity, wherein a radiologist examines the screening mammography image 10 in a step 20 and reports a set of suspicious regions 30 designated as S1. The CAD system then operates on the image 10 in a

step 40 and reports a set of suspicious regions 50 designated as S2. The radiologist then examines set S2 and accepts or rejects members of set S2 as suspicious in a step 60, thereby forming a third set of suspicious regions 70 denoted as S3, which is a subset of S2. The radiologist then creates in a step 80 a set of workup regions 90 denoted as S4 which is the union of sets S1 and S3. The workup regions 90 are then recommended for further examination such as taking additional mammograms with greater resolution, examining the areas of the breast tissue corresponding to the workup regions by means of ultrasound, or performing biopsies of the breast tissue.

Referring to Fig. 32, an alternative embodiment of the invention may be seen therein to include a density detector 800, a density classifier 900, and a detection results combiner 1000 in addition to the elements described above. The density detector 800 detects masses and lesions appearing in a digital representation of a screening mammogram. The density classifier 900 classifies detected densities by means of an MLP NN as either suspicious or not suspicious in a manner similar to the MLP NN described above with respect to the microcalcification classifier. The detected densities classified as suspicious are then fused together and combined with the suspicious detected microcalcifications in the detection results combiner 1000.

While the invention has been described in connection with detecting clustered microcalcifications in mammograms, it should be understood that the methods and systems described herein may also be applicable to other medical images such as chest x-rays.

While the form of apparatus herein described constitutes a preferred embodiment of this invention, it is to be understood that the invention is not limited to this precise form of apparatus, and that changes may be made therein without departing from the scope of the invention which is defined in the appended claims.

What is claimed is:

1. A method for automated detection of clustered microcalcifications from a digital mammogram comprising the steps of:

obtaining a digital mammogram;

optimizing first parameters for cropping said digital mammogram;

cropping said digital mammogram, based on said optimized first parameters, to produce a cropped image representative of breast tissue in said digital mammogram;

optimizing second parameters for detecting clustered microcalcifications in said cropped image;

detecting clustered microcalcifications in said cropped image based on said optimized second parameters;

indicating the position of said detected clustered microcalcifications in said digital mammogram.

2. A method for segmenting an area of a digital mammogram image corresponding to breast tissue from the remainder of the image, comprising the steps of:

storing a digital representation of said digital mammogram image;

enhancing the histogram of the digital representation to produce an enhanced image in which the contrast of the area of the mammogram image corresponding to breast tissue is increased;

thresholding the enhanced image to produce a binary image comprising a seed pixel;

region growing said seed pixel in said binary image to produce a mask;

closing holes in said mask;

eroding said mask;

dilating said mask; and

cropping said digital representation to the size of the largest object in said mask.

3. A method for detecting clustered microcalcifications in a digital mammogram

image comprising the steps of:

first filtering said digital mammogram image to reduce noise in said image to produce a noise-reduced image;

second filtering said noise-reduced image with a difference of Gaussians filter to produce a DoG-filtered image in which the appearance of potential microcalcifications has been enhanced;

globally thresholding said DoG-filtered image to segment potential microcalcifications from said DoG-filtered image;

locally thresholding said DoG-filtered image to segment potential microcalcifications from said DoG-filtered image;

logically ANDing together the globally and locally thresholded potential microcalcifications;

converting the logically ANDed potential microcalcifications to single-pixel coordinate representations;

removing single-pixel coordinate representations lying outside the area of the digital mammogram image corresponding to breast tissue;

clustering together the single-pixel coordinate representations remaining from the previous step to identify potential clustered microcalcifications;

computing features for each of the potential clustered microcalcifications;

eliminating potential clustered microcalcifications based on the computed features for each of the potential clustered microcalcifications; and

indicating in the digital mammogram image the locations of those potential clustered microcalcifications remaining after the previous step.

4. A method for automated clustered microcalcification detection by digital image processing in screening mammography, comprising:

storing a digital representation of a mammogram;

convolving a filter kernel comprising a difference-of-Gaussians equation with said digital representation, whereby information in the image which does not conform to the size and shape characteristics of a microcalcification is suppressed and suspected microcalcifications appear as bright spots in a resulting image; and

locally and globally thresholding said resulting image, whereby a second resulting image is obtained that essentially comprises only areas of suspected microcalcifications.

5. A method for automated clustered microcalcification detection by digital image processing in screening mammography, comprising:

storing a digital representation of a mammogram;

using an optimizing algorithm and a database of training images to obtain optimized parameter values; and

applying a filtering algorithm using said optimized parameters to said digital representation to obtain a filtered image essentially comprising suspected microcalcifications;

shrinking said filtered image to obtain an image essentially comprising single-pixel representations of said suspected microcalcifications;

grouping said single-pixel representations into clusters using said optimized parameters.

6. The method according to claim 5, wherein said step of using an optimizing algorithm comprises:

using a genetic algorithm.

7. The method according to claim 6, wherein:

said step of using a genetic algorithm comprises obtaining a d_{nn} value and a μCs_{min} value where d_{nn} represents a nearest neighbor distance and μCs_{min} represents a number of detected microcalcifications; and

said step of grouping groups single-pixel representations into clusters which represent microcalcifications that are within the distance d_{nn} of μCs_{min} other microcalcifications.

8. The method according to claim 7, wherein said step of using a genetic algorithm further comprises the step of:

iteratively searching a solution space containing possible values for d_{nn} and μCs_{min} to identify sets of values in which at least one fitness function is maximized.

9. The method according to claim 8, wherein said step of using a genetic algorithm comprises the step of:

using a simplex method to identify at least one of said sets of values in which a cost function is minimized.

10. A method for automated clustered microcalcification detection by digital image processing in screening mammography, comprising:

storing a digital representation of a mammogram;

locating potential clusters of microcalcifications in said digital representation;

extracting features of said potential clusters of microcalcifications;

using said extracted features as inputs to a multi-layer perceptron artificial neural network; and

using said multi-layer perceptron artificial neural network to classify said clusters of microcalcifications as suspicious or non-suspicious.

11. The method according to claim 10, wherein said step of using said multi-layer perceptron artificial neural network to classify said clusters of microcalcifications as suspicious or non-suspicious comprises:

using output values of said multi-layer perceptron artificial neural network in a smoothly varying output function to obtain a series of resulting values; and

classifying a cluster associated with one of said resulting values as suspicious if that value is greater than or equal to a threshold value, or non-suspicious if that value is less than said threshold value.

12. The method according to claim 11, wherein said smoothly varying output function comprises a hyperbolic tangent function.

13. The method according to claim 11, wherein said smoothly varying output

function comprises a linear function.

14. The method according to claim 11, wherein said smoothly varying output function comprises a sigmoid function.

15. The method according to claim 11, wherein said step of using said multi-layer perceptron artificial neural network to classify said clusters of microcalcifications as suspicious or non-suspicious comprises:

multiplying at least one of said features by a weight $w_{i,j}$, where I is an index representing the i^{th} feature vector element of a feature vector x having N elements and j is an index representing a j^{th} first layer node; and

using first layer nodes of said multi-layer perceptron artificial neural network to calculate first layer outputs f_j, said first layer outputs f_j being calculated according to the function:

$$f_j = \tanh\left(\sum_{i=1}^{N}(w_{i,j} \times x_i)\right)$$

where x_i comprises a computed feature vector element.

16. The method according to claim 15, wherein said step of using said multi-layer perceptron artificial neural network to classify said clusters of microcalcifications as suspicious or non-suspicious further comprises:

multiplying at least one of said first layer outputs f_j by a second weight $u_{j,k}$; and

using a result of said multiplying step as an input to at least one output node, the output of said at least one output node being calculated according to the function:

$$z_k(y) = \tanh\left(\sum_{j=1}^{J}(u_{j,k} \times y_j)\right)$$

where $y_j = f_j(x)$, k is an index representing the k^{th} output node, and J is the number of first layer outputs to be multiplied.

17. A method for incorporating the output detections of a computer-aided detection system for detecting clustered microcalcifications in a mammogram with observed detections of a human interpreter of the same mammogram without reducing sensitivity, comprising:

obtaining said observed detections to form a first set of detections;

obtaining said output detections to form a second set of detections;

accepting some output detections in said second set to form a third set of detections;

combining said first set and said third set to form a fourth set of detections; and

providing an output based on said fourth set of detections.

18. A method for automated clustered microcalcification detection by digital image processing in screening mammography, comprising:

storing a digital representation of a mammogram;

filtering said digital representation to obtain a filtered image comprising suspected microcalcifications;

thresholding said filtered image with a sloping local threshold to obtain an image that essentially comprises only areas of suspected microcalcifications.

19. The method according to claim 18, wherein said step of thresholding comprises:

centering a window over a pixel of interest having coordinates (x,y) is said digital representation;

computing the mean (x,y) and standard deviation (x,y) of the pixels under said window;

computing a local threshold value T(x,y) for said pixel of interest according to the function:

$$T(x,y) = A + B\mu(x,y) + C\sigma(x,y)$$

where A is a predetermined offset and B and C are predetermined coefficients;

comparing the gray-scale value of the corresponding pixel of interest in said filtered image to said local threshold value; and

generating a binary image by setting a corresponding pixel in said binary image to a one if said gray-scale value is greater than or equal to said local threshold, and to a zero if said gray-scale value is less than said local threshold.

20. An apparatus for automated detection of clustered microcalcifications from a digital mammogram comprising:

means for obtaining a digital mammogram;

means for optimizing first parameters for cropping said digital mammogram;

means for cropping said digital mammogram, said means for cropping using said optimized first parameters to produce a cropped image representative of breast tissue in said digital mammogram;

means for optimizing second parameters for detecting clustered microcalcifications in said cropped image;

means for detecting clustered microcalcifications in said cropped image using said optimized second parameters;

means for indicating the positions of said detected clustered microcalcifications in said digital mammogram.

21. An apparatus for detecting clustered microcalcifications in a digital mammogram image comprising:

a difference of Gaussians filter for producing a DoG-filtered image in which the appearance of potential microcalcifications has been enhanced;

thresholding means for segmenting said potential microcalcifications from said DoG-filtered image;

extracting means for generating single-pixel coordinate representations for said potential microcalcifications; and

clustering means for grouping said single-pixel representations into clusters.

22. An apparatus for automated clustered microcalcification detection by digital image processing in screening mammography comprising:

means for storing a digital representation of a mammogram;

means for convolving a filter kernel comprising a difference-of-Gaussians equation with said digital representation, whereby information in the image which does not conform to the size and shape of a microcalcification is suppressed and suspected microcalcifications appear as bright spots in a resulting image; and

means for locally and globally thresholding said resulting image, whereby a second resulting image is obtained that essentially comprises only areas of suspected microcalcifications.

23. An apparatus for automated clustered microcalcification detection by digital image processing in screening mammography comprising:

means for storing a digital representation of a mammogram;

means for optimizing parameter values using an optimizing algorithm and a database of training images;

means for applying a filtering algorithm, using said optimized parameters, to said digital representation to obtain a filtered image essentially comprising suspected microcalcifications;

means for shrinking said filtered image to obtain an image essentially comprising single-pixel representations of said suspected microcalcifications; and

means for grouping said single-pixel representations into clusters using said optimized parameters.

24. The apparatus according to claim 23 wherein said optimizing algorithm is a genetic algorithm.

25. The apparatus according to claim 24 wherein said means for optimizing parameter values comprises:

means for obtaining a d_{nn} value and a μCs_{min} value where d_{nn} represents a nearest neighbor distance and μCs_{min} represents a number of detected

microcalcifications; and

wherein said means for grouping groups said single-pixel representations into clusters which represent microcalcifications that are within the distance d_{nn} of μCs_{min} other microcalcifications.

26. The apparatus according to claim 25 wherein said means for optimizing parameters comprises:

means for iteratively searching a solution space containing possible values for d_{nn} and μCs_{min} to identify sets of values in which at least one fitness function is maximized.

27. The apparatus according to claim 26 wherein said means for optimizing parameters comprises:

means for using a simplex method to identify at least one of said sets of values in which a cost function is minimized.

28. An apparatus for automated clustered microcalcification detection by digital image processing in screening mammography comprising:

means for storing a digital representation of a mammogram;

means for locating potential clusters of microcalcifications in said digital representation;

means for extracting features of said potential clusters of microcalcifications;

means for classifying said potential clusters of microcalcifications as suspicious or non-suspicious using said features.

29. The apparatus according to claim 28 wherein said means for classifying comprises a multi-layer perceptron artificial neural network.

30. The apparatus according to claim 29 wherein said multi-layer perceptron neural network comprises:

smoothly varying output means.

31. The apparatus according to claim 30 wherein said smoothly varying output means comprises:

means for applying a hyperbolic tangent function to a sum of weighted inputs to provide an output indicative of whether a clustered microcalcification is suspicious or non-suspicious.

32. The apparatus according to claim 30 wherein said smoothly varying output means comprises:

means for applying a sigmoid function to a sum of weighted inputs to provide an output indicative of whether a clustered microcalcification is suspicious or non-suspicious.

33. The apparatus according to claim 30 wherein said smoothly varying output means comprises:

means for applying a linear function to a sum of weighted inputs to provide an output indicative of whether a clustered microcalcification is suspicious or non-suspicious.

34. The apparatus according to claim 30 wherein said multi-layer perceptron artificial neural network comprises:

means for multiplying at least one of said features by a weight w_{ij}, where i is an index representing the ith feature vector element of a feature vector x having N elements and j is an index representing a jth first layer node; and

first layer nodes for calculating first layer outputs f_j according to the function:

$$f_j = \tanh\left(\sum_{i=1}^{N}(w_{i,j} \times x_i)\right)$$

where x_i comprises a computed feature vector element.

35. The apparatus according to claim 34, wherein said multi-layer perceptron

artificial neural network further comprises:

means for multiplying at least one of said first layer outputs f_j by a second weight $u_{j,k}$; and

at least one output node for calculating outputs z_k, where k is an index representing a k^{th} output node, according to the function:

$$z_k(y) = \tanh\left(\sum_{j=1}^{J} (u_{j,k} \times y_j)\right)$$

where $y_j = f_j(x)$ and J is the number of first layer outputs to be multiplied.

36. A method for automated clustered microcalcification and density detection by digital image processing in screening mammography, comprising:

storing a digital representation of a mammogram;

convolving a filter kernel comprising a difference-of-Gaussians equation with said digital representation, whereby information in the image which does not conform to the size and shape characteristics of a microcalcification is suppressed and suspected microcalcifications appear as bright spots in a resulting image;

thresholding said first resulting image, whereby a second resulting image is obtained that essentially comprises only areas of suspected microcalcifications;

detecting densities in said digital representation; and

producing a third resulting image that comprises only areas of suspected densities.

37. A method for automated image cropping by digital image processing in screening mammography, comprising:

storing a first digital representation of a mammogram;

dilating said first digital representation to produce a dilated digital representation;

cropping said dilated digital representation to the size of the largest contiguous group of pixels, whereby a cropped dilated digital representation is produced; and

selecting for subsequent processing pixels in said first digital representation which correspond to pixels in said cropped dilated digital representation.

38. A method for automated microcalcification detection by digital image processing in screening mammography, comprising:

storing a digital representation of a mammogram;

normalizing brightness values of said digital representation;

using a predetermined contrast setting in a region growing algorithm to create a breast mask which defines an area of said digital representation containing breast tissue; and

searching said area containing breast tissue for microcalcifications.

39. The method according to claim 38, wherein said step of normalizing comprises a step of histogram equalization.

40. A method for automated microcalcification detection by digital image processing in screening mammography, comprising:

storing a digital representation of a mammogram;

searching a region of said digital representation to find a seed pixel;

using a region-growing algorithm to create a breast mask which defines an area of said digital representation containing breast tissue, said step of using a region-growing algorithm further comprising:

using a region-growing function which begins at said seed pixel and progressively groups together nearest neighbor pixels which share a characteristic, whereby a contiguous group of pixels is created;

using said contiguous group of pixels to determine a breast mask which defines an area of said digital representation containing breast tissue; and

searching said area containing breast tissue for microcalcifications.

41. The method according to claim 40, wherein said step of searching a region of said digital representation to find a seed pixel comprises finding a pixel within said

region which has a maximum gray-scale value.

42. The method according to claim 40, wherein said step of grouping together nearest neighbor pixels sharing a characteristic comprises determining whether each nearest neighbor pixel has a contrast ratio which is less than a contrast ratio threshold.

43. A method for automated microcalcification detection by digital image processing in screening mammography, comprising:

storing a digital representation of a mammogram;

computing a local threshold value from pixels in said digital representation;

filtering said digital representation using a difference-of-gaussians filter to create a filtered image;

creating a thresholded image by comparing pixels in said filtered image to said local threshold value and adjusting pixel values in accordance with a result of said comparison; and

further processing said thresholded image to identify microcalcifications.

44. A method for automated microcalcification detection by digital image processing in screening mammography, comprising:

storing a digital representation of a mammogram;

using a genetic algorithm and a database of training images to obtain a value of at least one parameter; and

using said at least one parameter in a function which processes said digital representation to identify microcalcifications.

45. The method according to claim 44, wherein said at least one parameter comprises a d_{nn} value and a μCs_{min} value, where d_{nn} represents a nearest neighbor distance and μCs_{min} represents a number of detected microcalcifications, and wherein said function comprises grouping single-pixel representations into clusters which represent microcalcifications that are within the distance d_{nn} of μCs_{min} other

microcalcifications.

46. The method according to claim 44, wherein said at least one parameter comprises a target size used in a difference-of-gaussians filter.

47. The method according to claim 44, wherein said at least one parameter comprises at least one threshold value.

48. The method according to claim 44, wherein said at least one parameter comprises a neighborhood size.

49. The method according to claim 44, wherein said function comprises a sloping local threshold function.

50. The method according to claim 44, wherein said at least one parameter comprises a percentage of a histogram.

51. The method according to claim 47, wherein said at least one threshold value comprises upper and lower threshold values.

Fig. 1

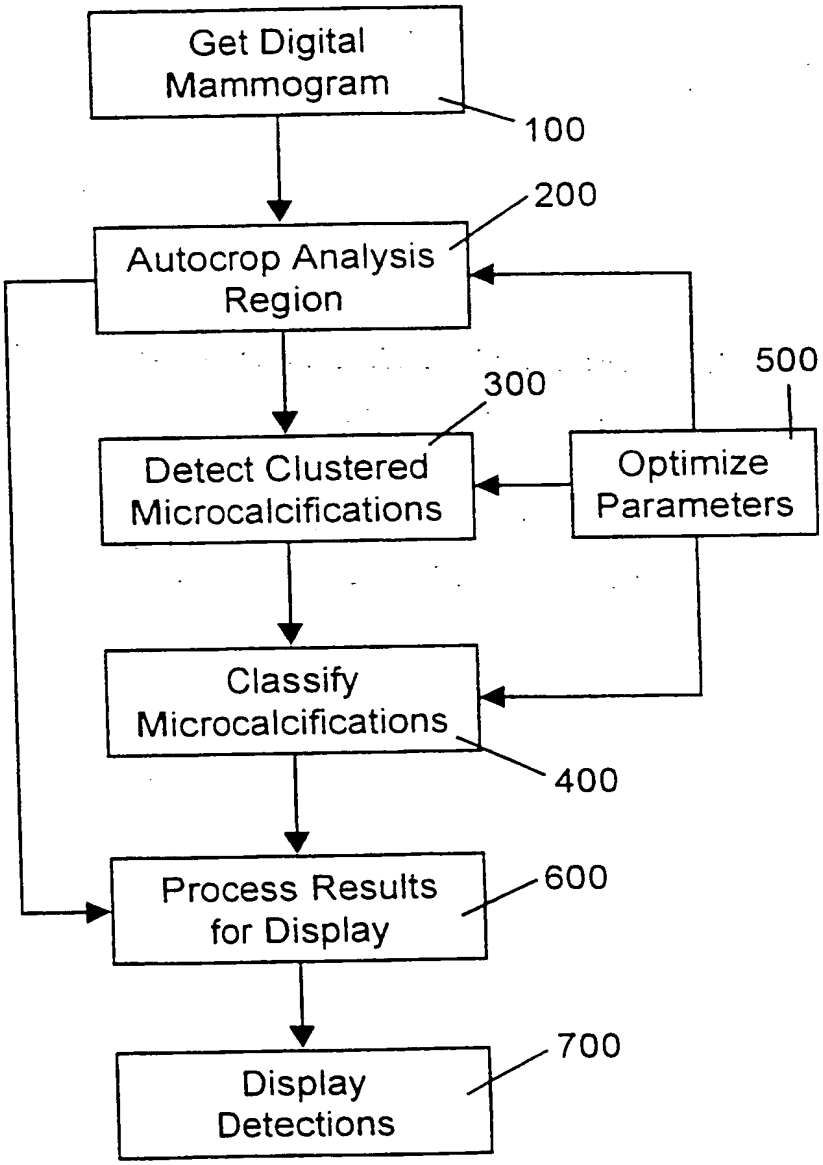
Get Digital Mammogram
100
200
Autocrop Analysis Region
500
300
Detect Clustered Microcalcifications
Optimize Parameters
Classify Microcalcifications
400
Process Results for Display
600
Display Detections
700

Fig. 2

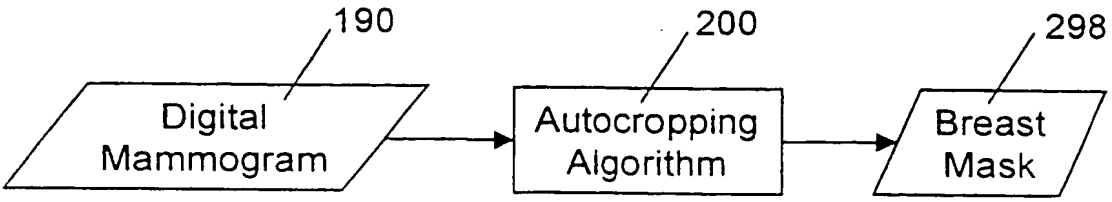
190
200
298
Digital Mammogram
Autocropping Algorithm
Breast Mask

Fig. 3

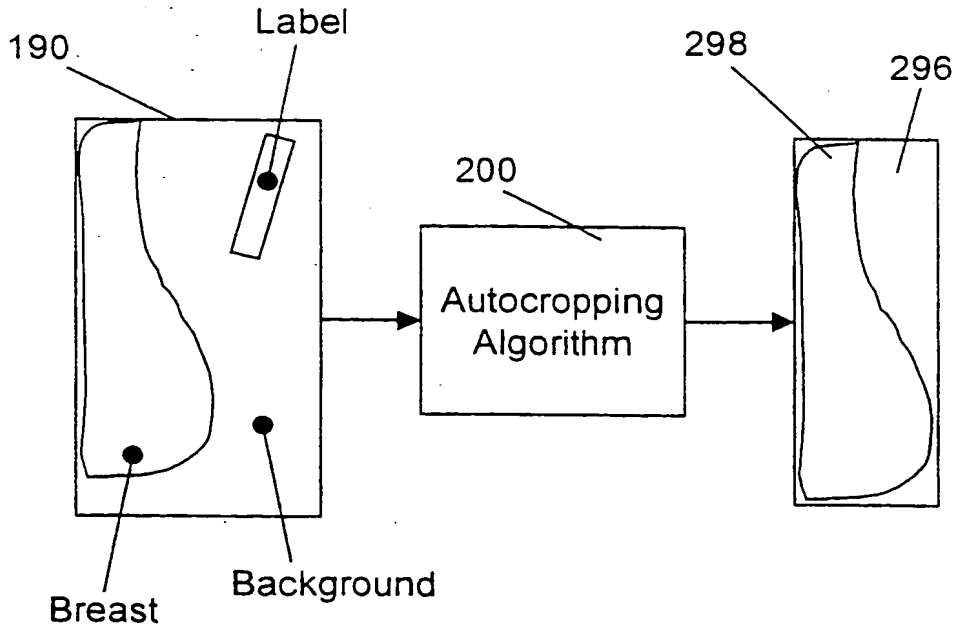
190
Label
298
296
200
Autocropping Algorithm
Breast
Background

Fig. 4

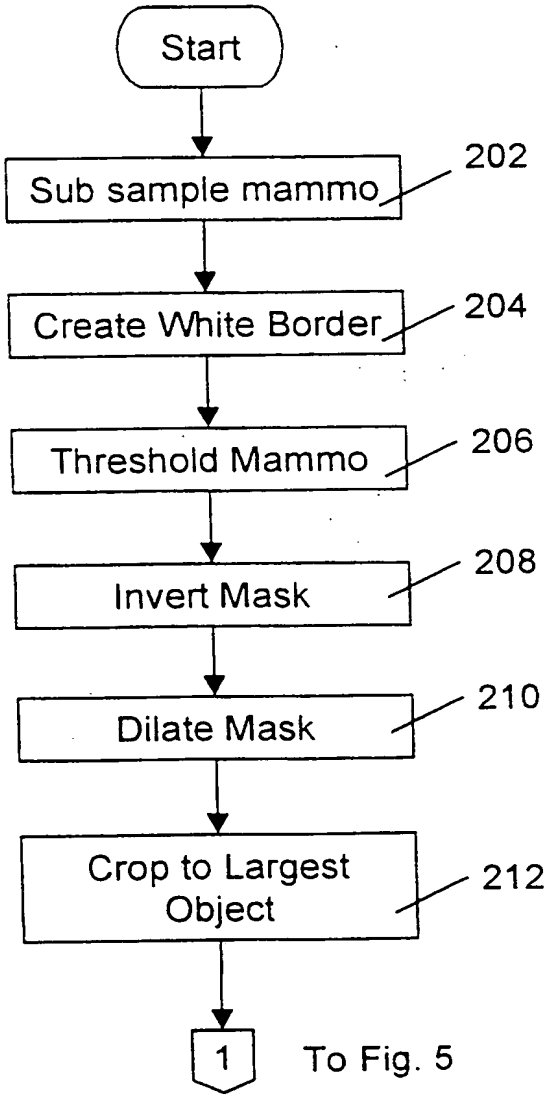
Start
Sub sample mammo
202
Create White Border
204
Threshold Mammo
206
Invert Mask
208
Dilate Mask
210
Crop to Largest Object
212
1
To Fig. 5

Fig. 5

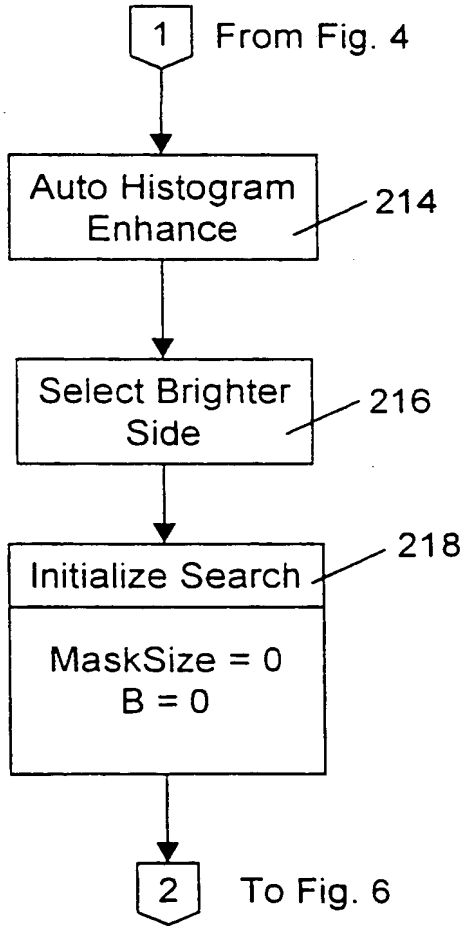
1
From Fig. 4
Auto Histogram Enhance
214
Select Brighter Side
216
Initialize Search
218
MaskSize = 0
B = 0
2
To Fig. 6

Fig. 6

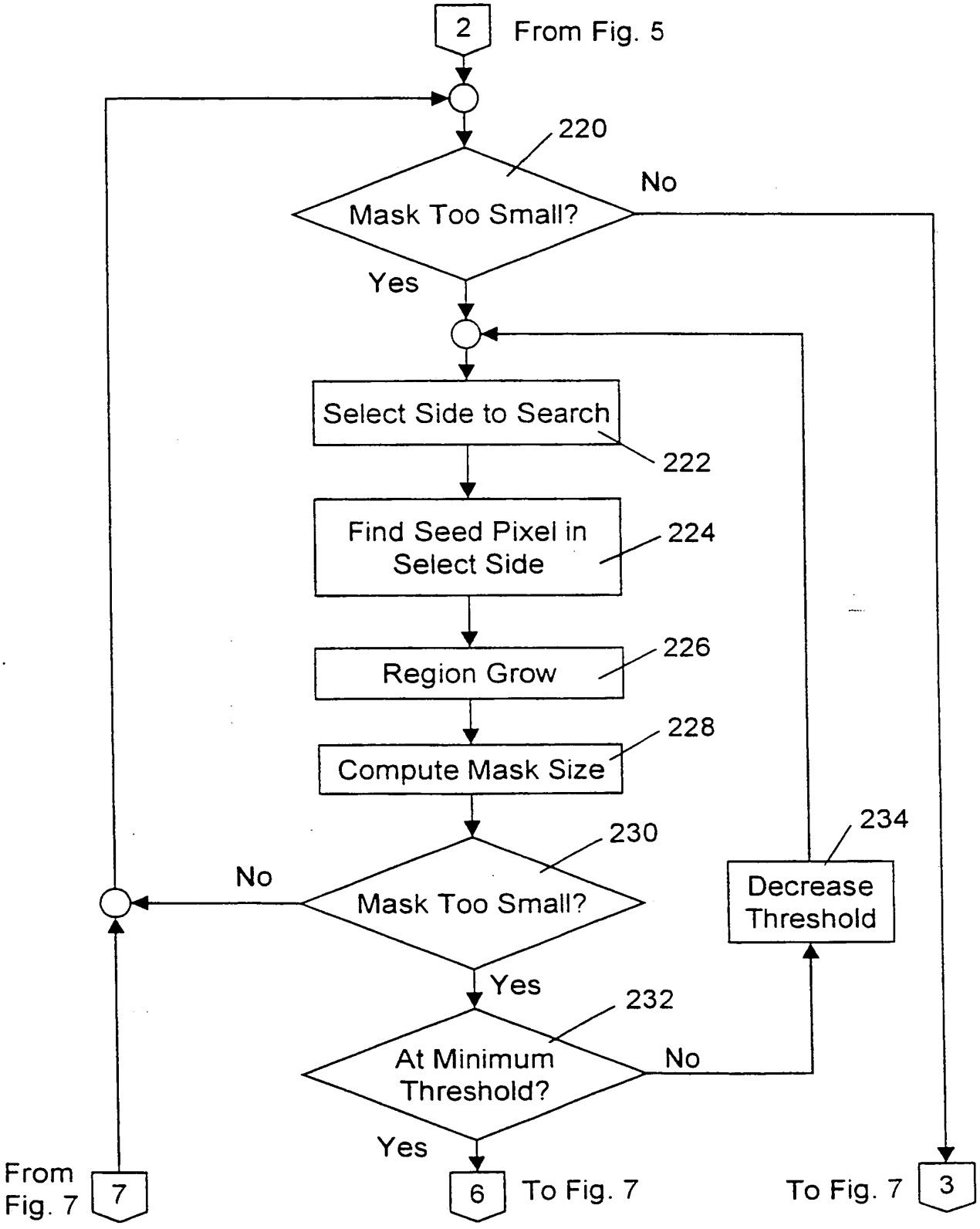
2
From Fig. 5
220
Mask Too Small?
No
Yes
Select Side to Search
222
Find Seed Pixel in Select Side
224
Region Grow
226
Compute Mask Size
228
230
Mask Too Small?
No
Yes
234
Decrease Threshold
232
At Minimum Threshold?
No
Yes
From Fig. 7
7
6
To Fig. 7
To Fig. 7
3

Fig. 7

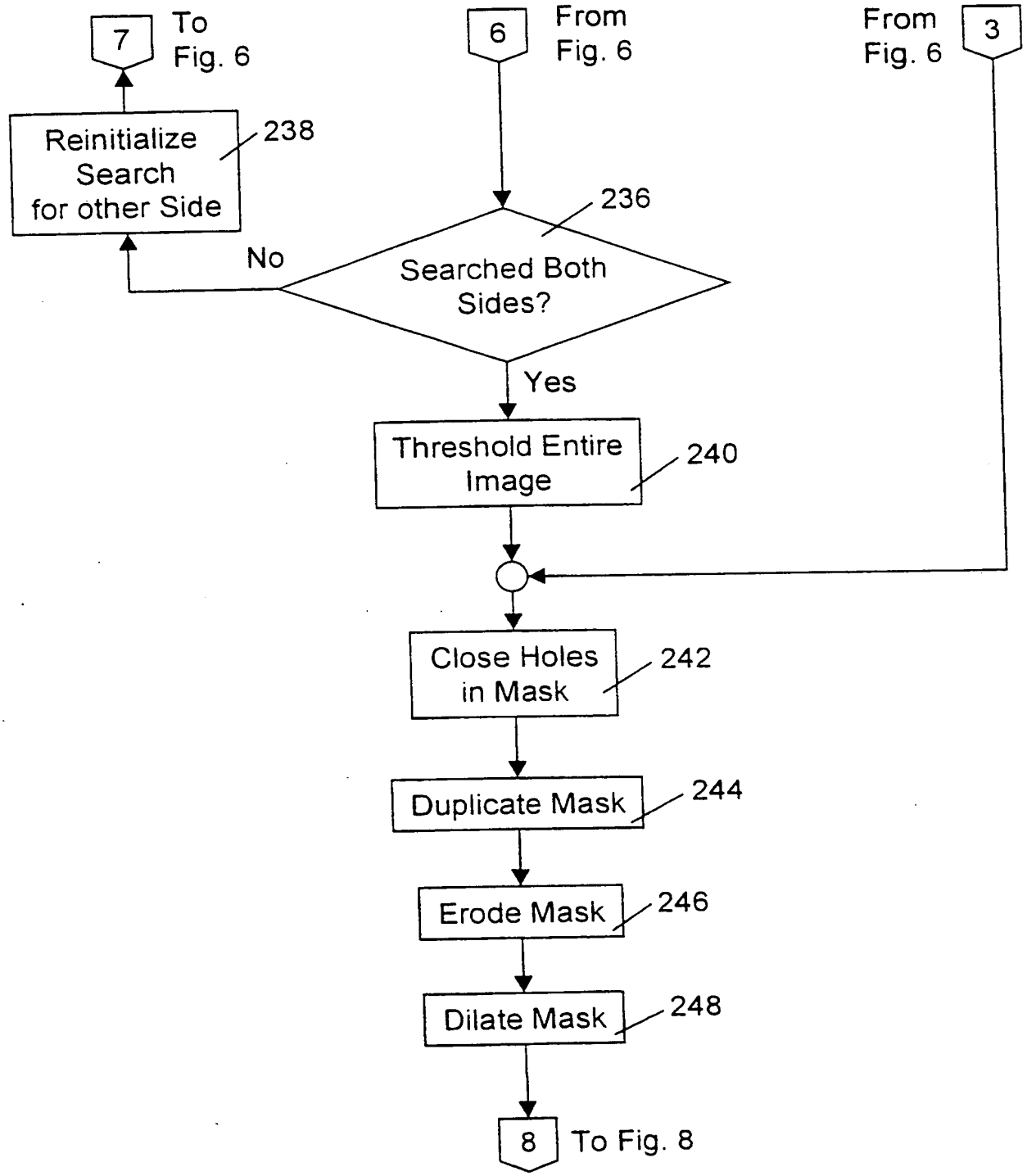
7
To Fig. 6
6
From Fig. 6
From Fig. 3
Reinitialize Search for other Side
238
236
No
Searched Both Sides?
Yes
Threshold Entire Image
240
Close Holes in Mask
242
Duplicate Mask
244
Erode Mask
246
Dilate Mask
248
8
To Fig. 8

Fig. 8

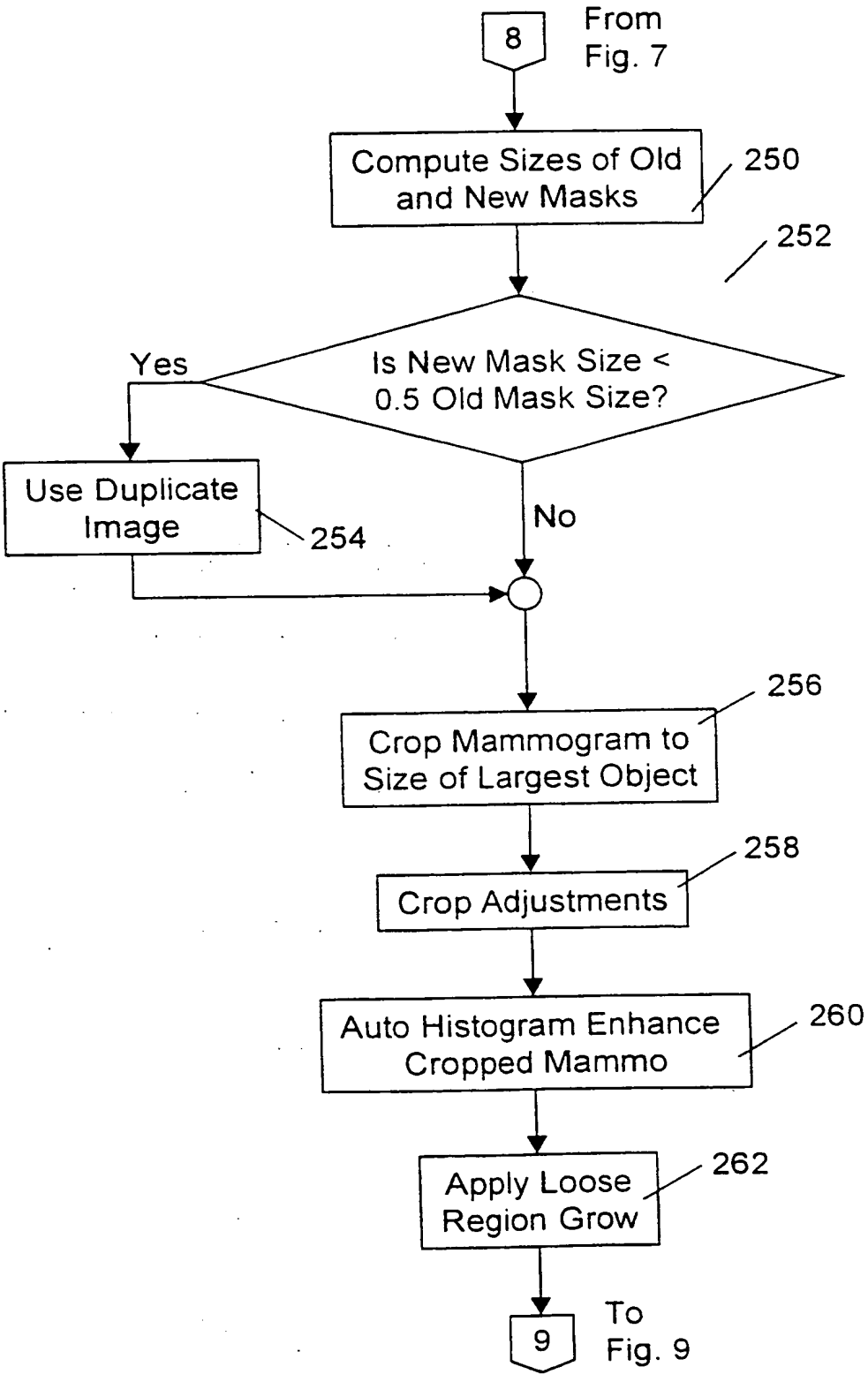
8
From Fig. 7
Compute Sizes of Old and New Masks
250
252
Is New Mask Size < 0.5 Old Mask Size?
Yes
No
Use Duplicate Image
254
256
Crop Mammogram to Size of Largest Object
258
Crop Adjustments
Auto Histogram Enhance Cropped Mammo
260
Apply Loose Region Grow
262
9
To Fig. 9

Fig. 9

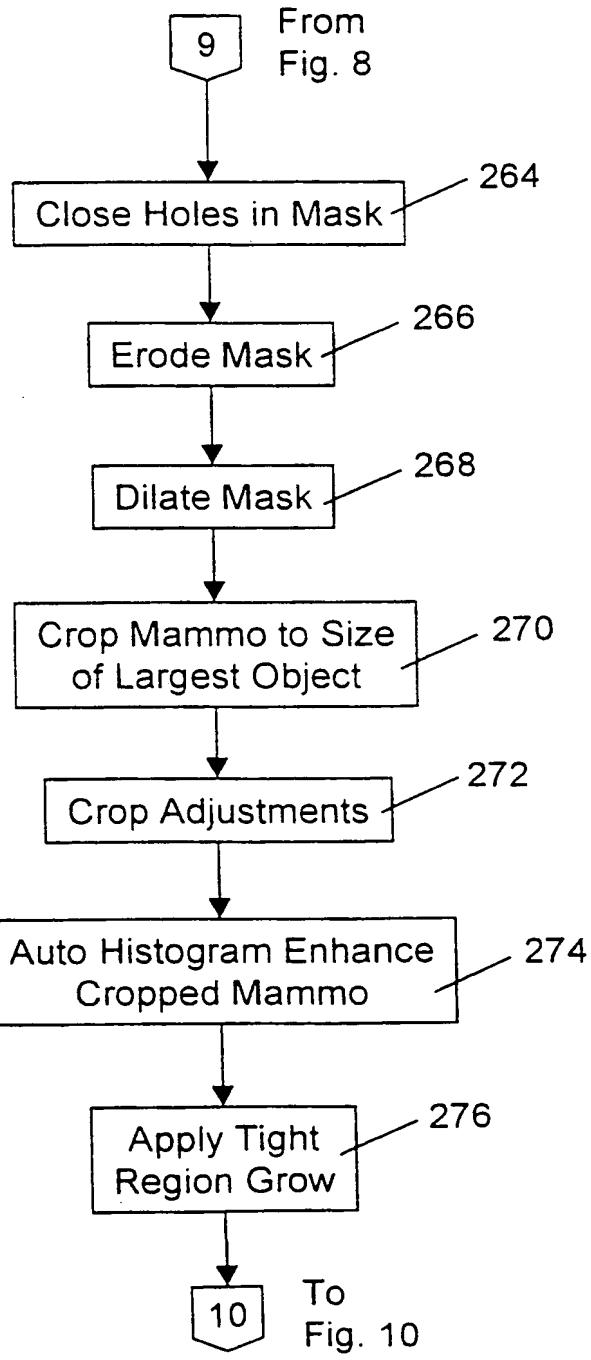
9
From Fig. 8
Close Holes in Mask
264
Erode Mask
266
Dilate Mask
268
Crop Mammo to Size of Largest Object
270
Crop Adjustments
272
Auto Histogram Enhance Cropped Mammo
274
Apply Tight Region Grow
276
10
To Fig. 10

Fig. 10

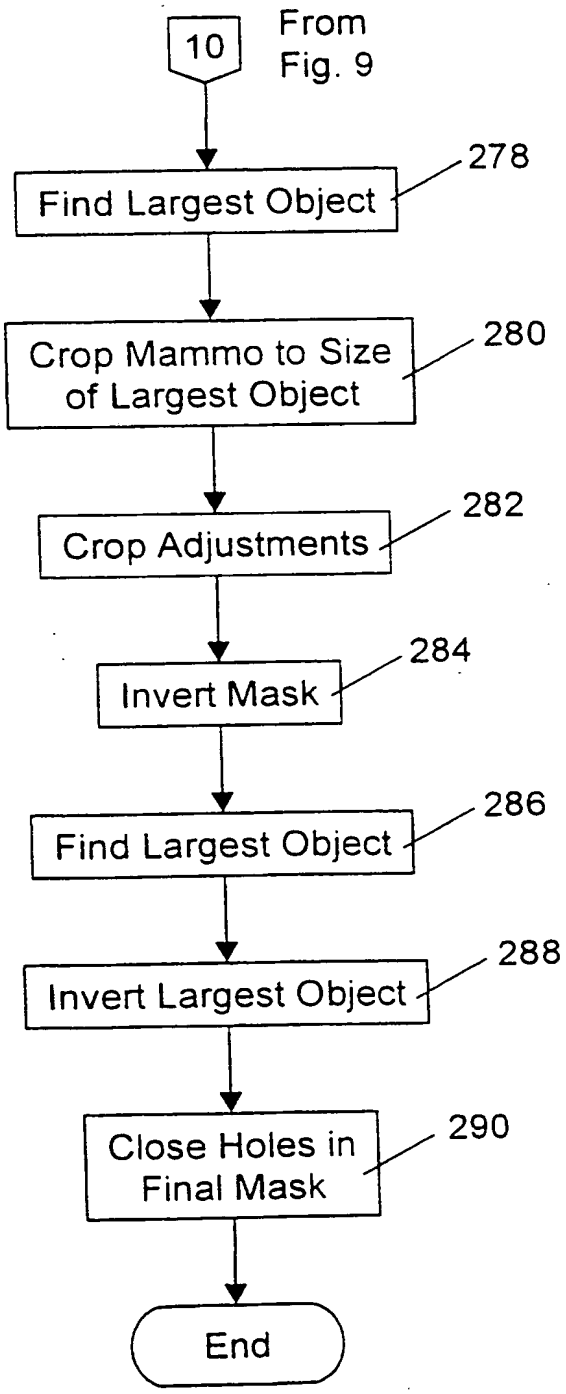
10
From Fig. 9
Find Largest Object
278
Crop Mammo to Size of Largest Object
280
Crop Adjustments
282
Invert Mask
284
Find Largest Object
286
Invert Largest Object
288
Close Holes in Final Mask
290
End

Fig. 11

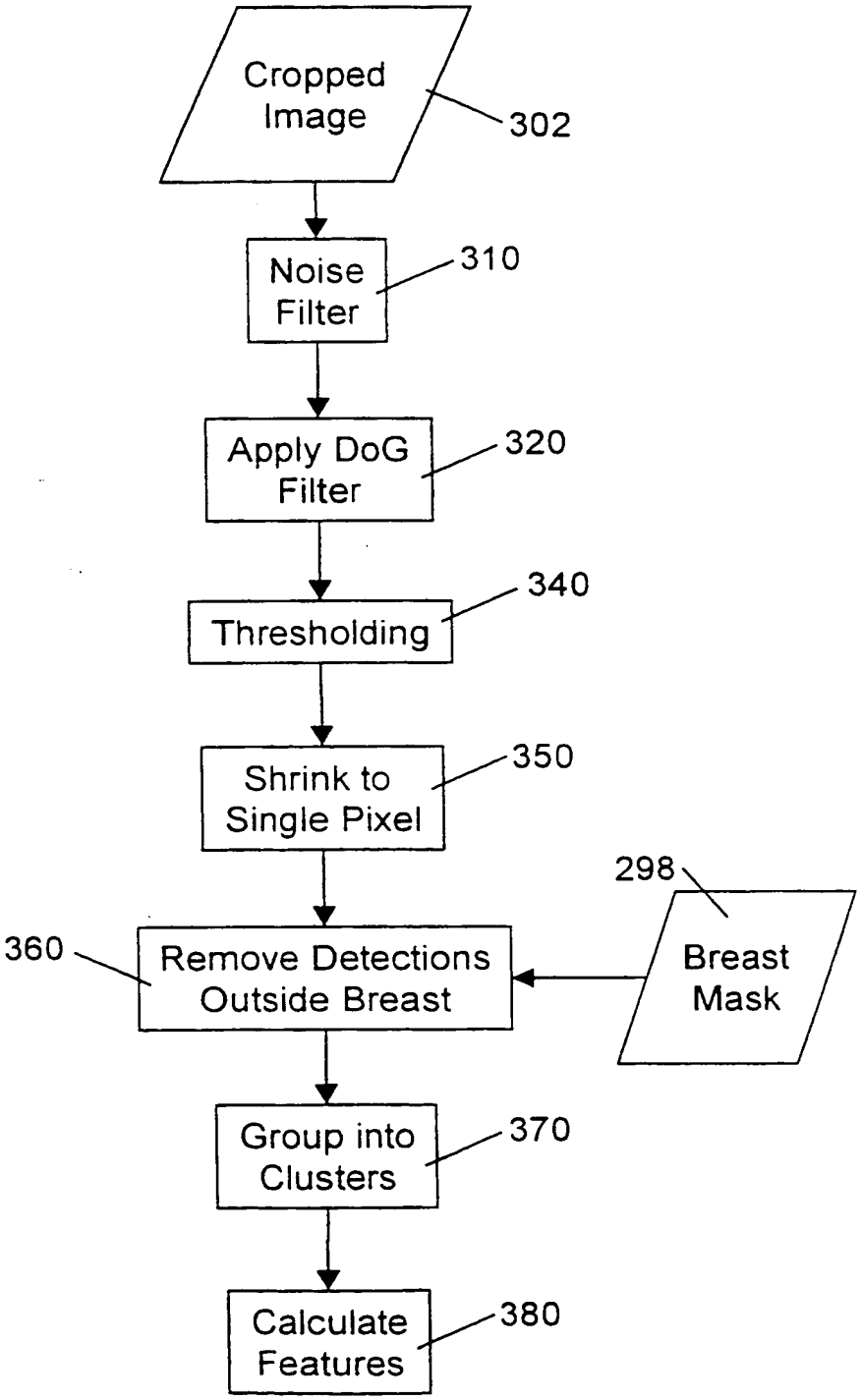
Cropped Image
302
Noise Filter
310
Apply DoG Filter
320
Thresholding
340
Shrink to Single Pixel
350
298
Breast Mask
360
Remove Detections Outside Breast
Group into Clusters
370
Calculate Features
380

Fig. 12

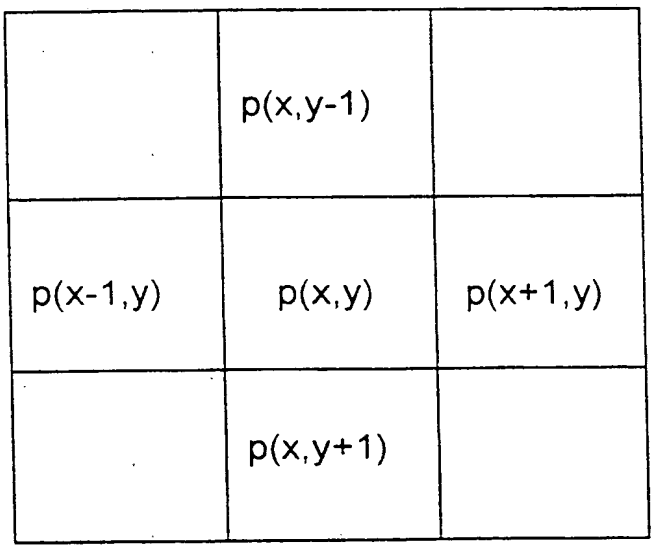

Fig. 13

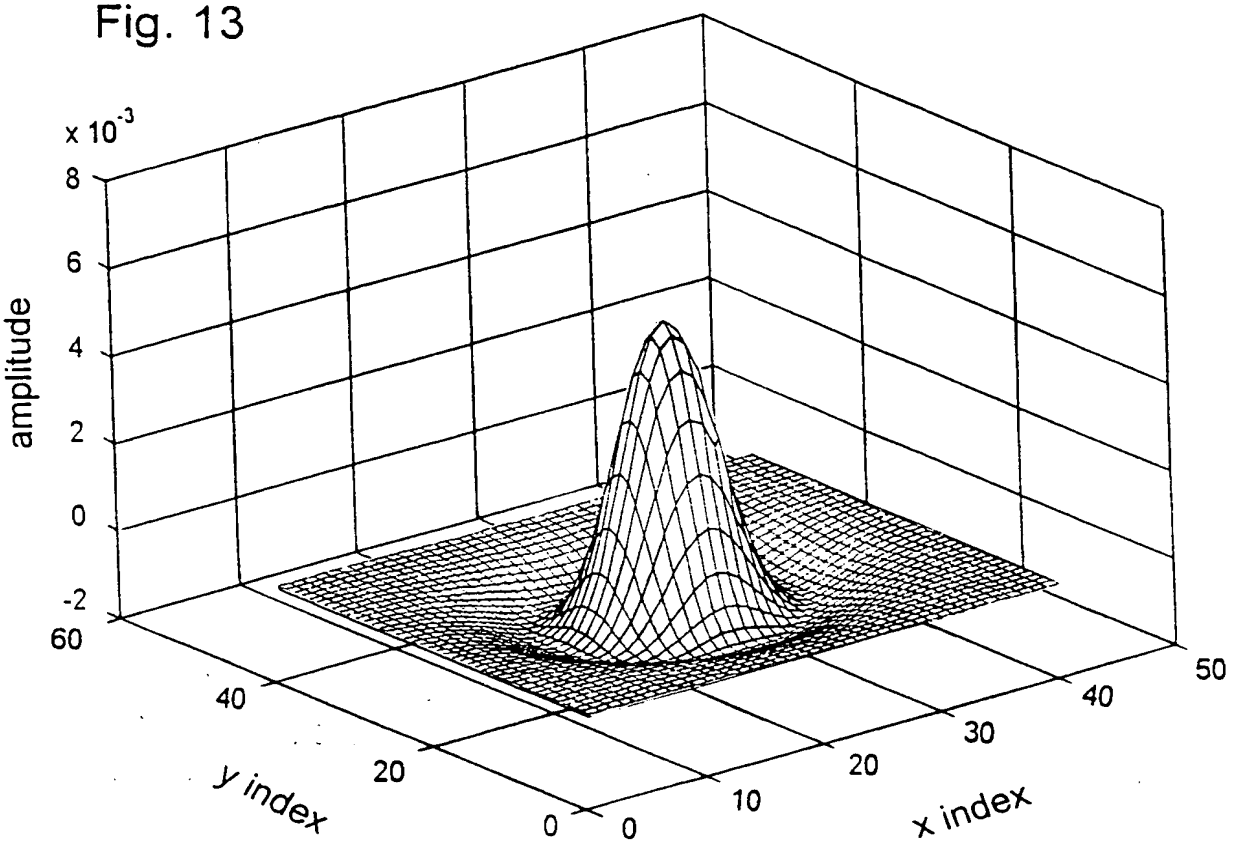
x 10^-3
8
6
4
2
0
-2
amplitude
60
40
20
0
y index
0
10
20
30
40
50
x index

Fig. 14

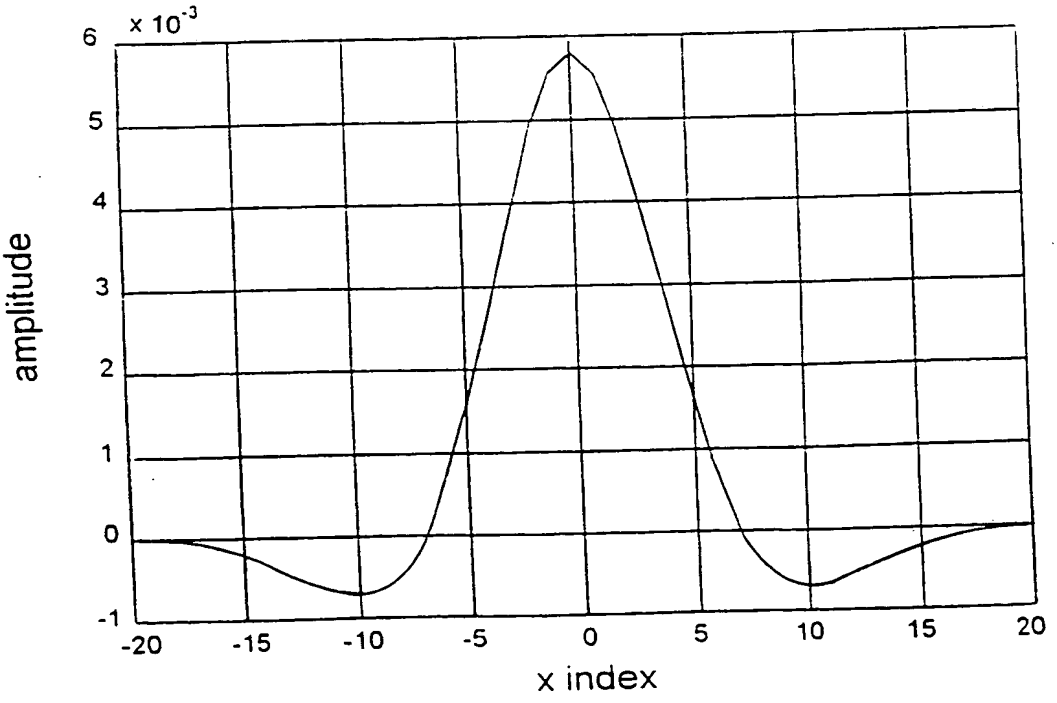
x 10^-3
6
5
4
3
2
1
0
-1
amplitude
-20
-15
-10
-5
0
5
10
15
20
x index

Fig. 15

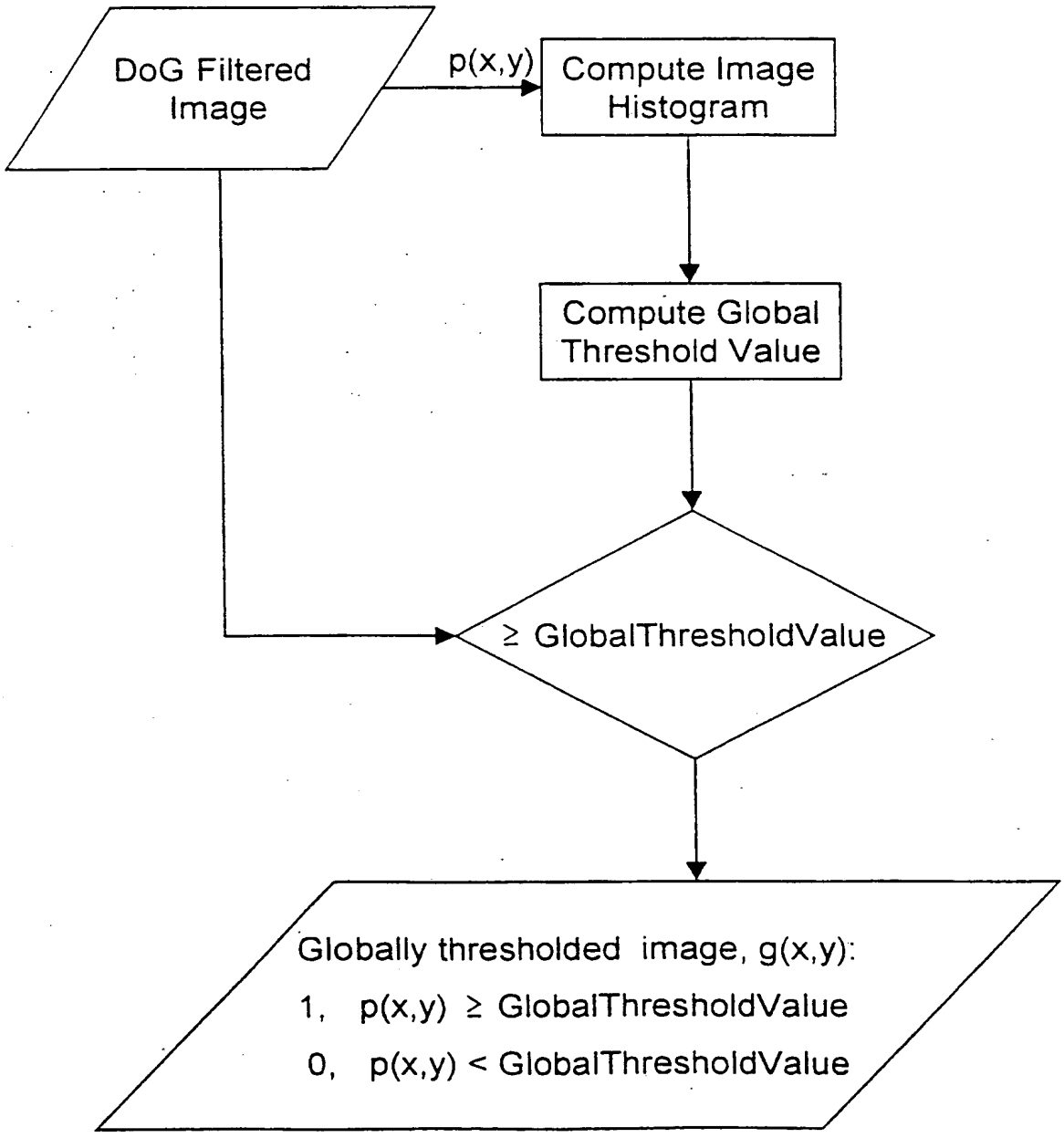
DoG Filtered Image
p(x,y)
Compute Image Histogram
Compute Global Threshold Value
≥ GlobalThresholdValue
Globally thresholded image, g(x,y):
1, p(x,y) ≥ GlobalThresholdValue
0, p(x,y) < GlobalThresholdValue

Fig. 16

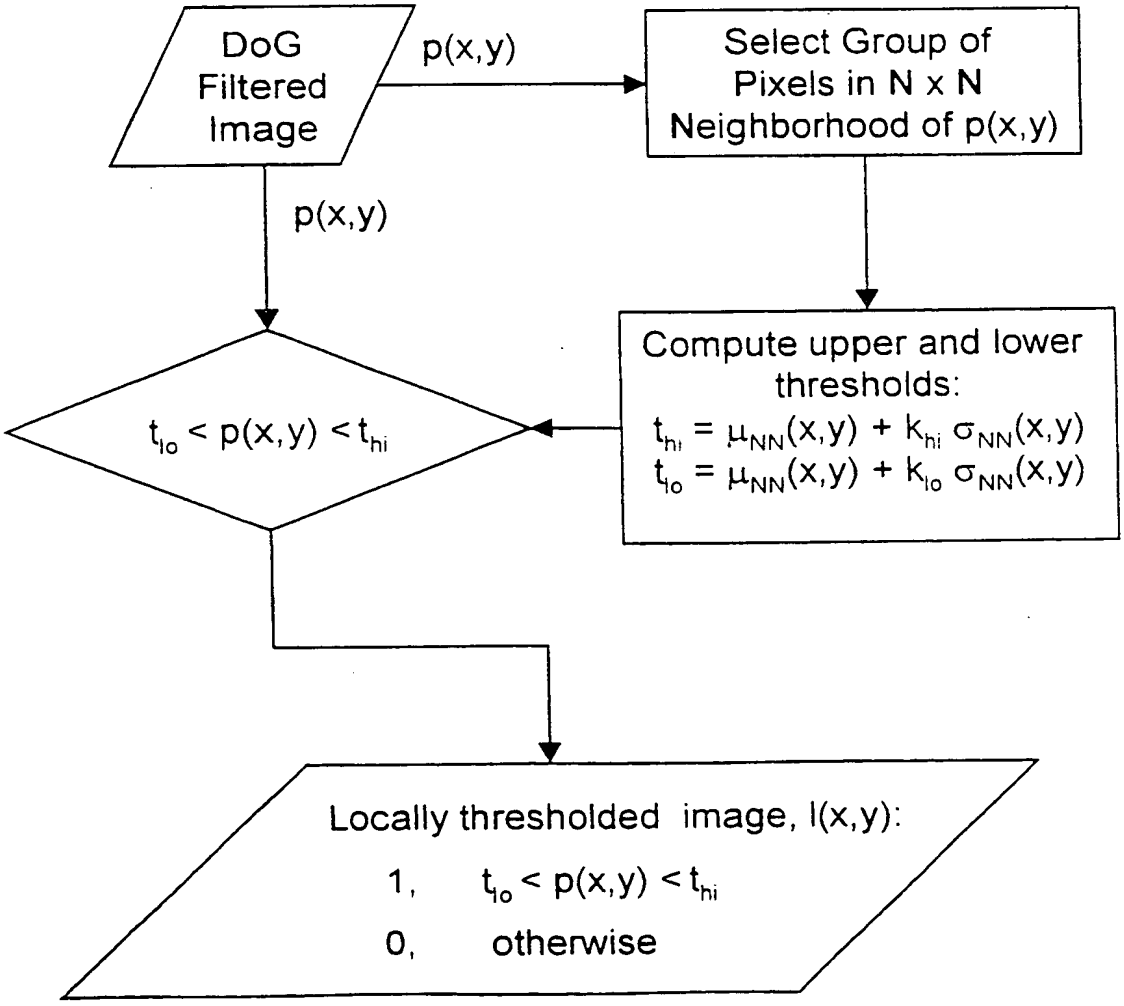
DoG Filtered Image
p(x,y)
Select Group of Pixels in N x N Neighborhood of p(x,y)
p(x,y)
Compute upper and lower thresholds:
$t_{hi} = \mu_{NN}(x,y) + k_{hi}\,\sigma_{NN}(x,y)$
$t_{lo} = \mu_{NN}(x,y) + k_{lo}\,\sigma_{NN}(x,y)$
$t_{lo} < p(x,y) < t_{hi}$
Locally thresholded image, I(x,y):
1, $t_{lo} < p(x,y) < t_{hi}$
0, otherwise

Fig. 17

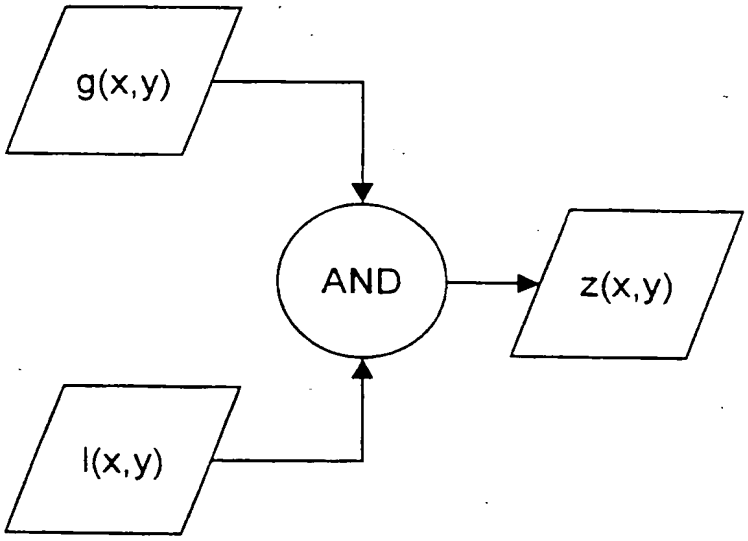

Fig. 18

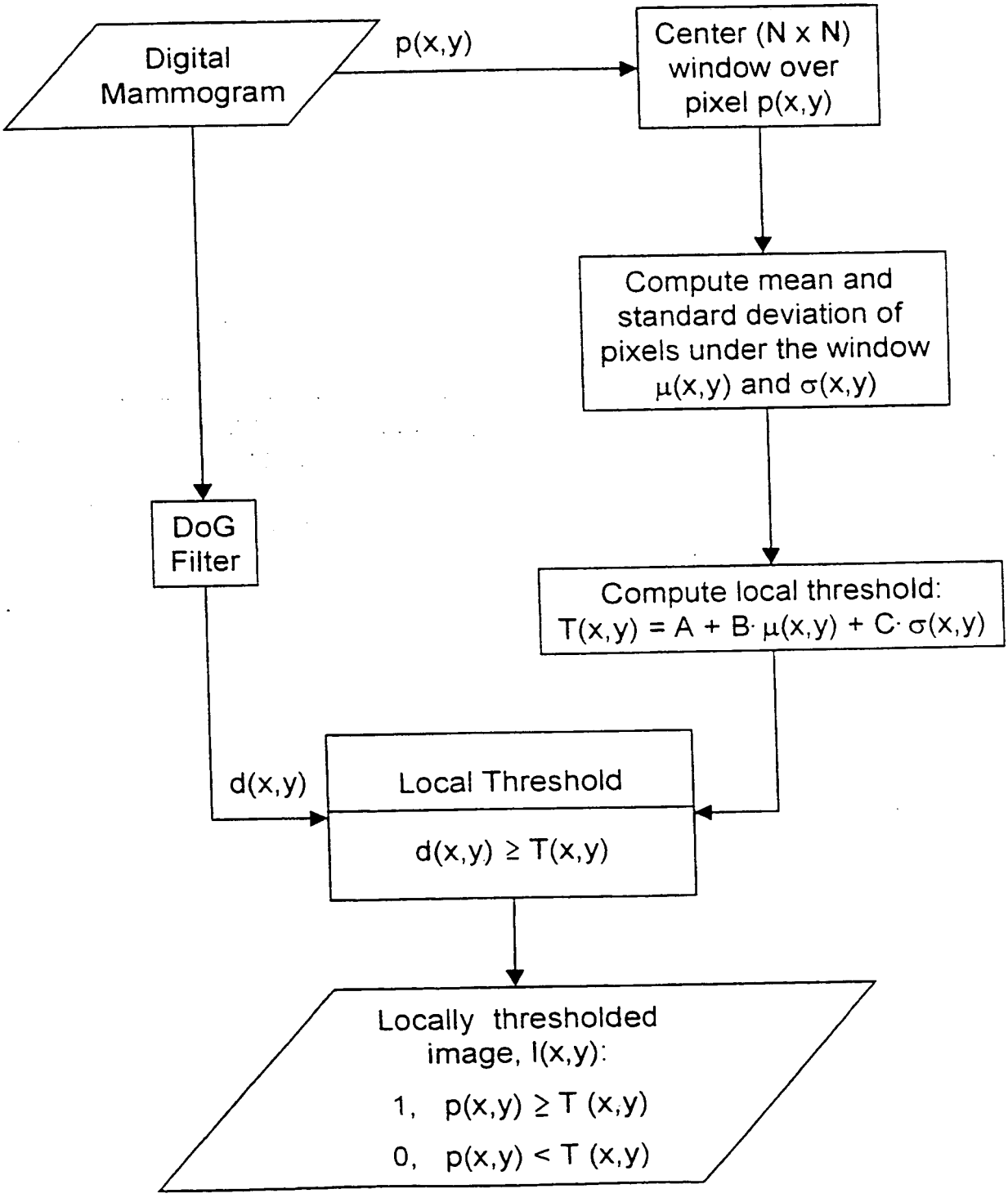
Digital Mammogram
p(x,y)
Center (N x N) window over pixel p(x,y)
Compute mean and standard deviation of pixels under the window μ(x,y) and σ(x,y)
DoG Filter
Compute local threshold: T(x,y) = A + B· μ(x,y) + C· σ(x,y)
d(x,y)
Local Threshold
d(x,y) ≥ T(x,y)
Locally thresholded image, I(x,y):
1, p(x,y) ≥ T (x,y)
0, p(x,y) < T (x,y)

Fig. 19

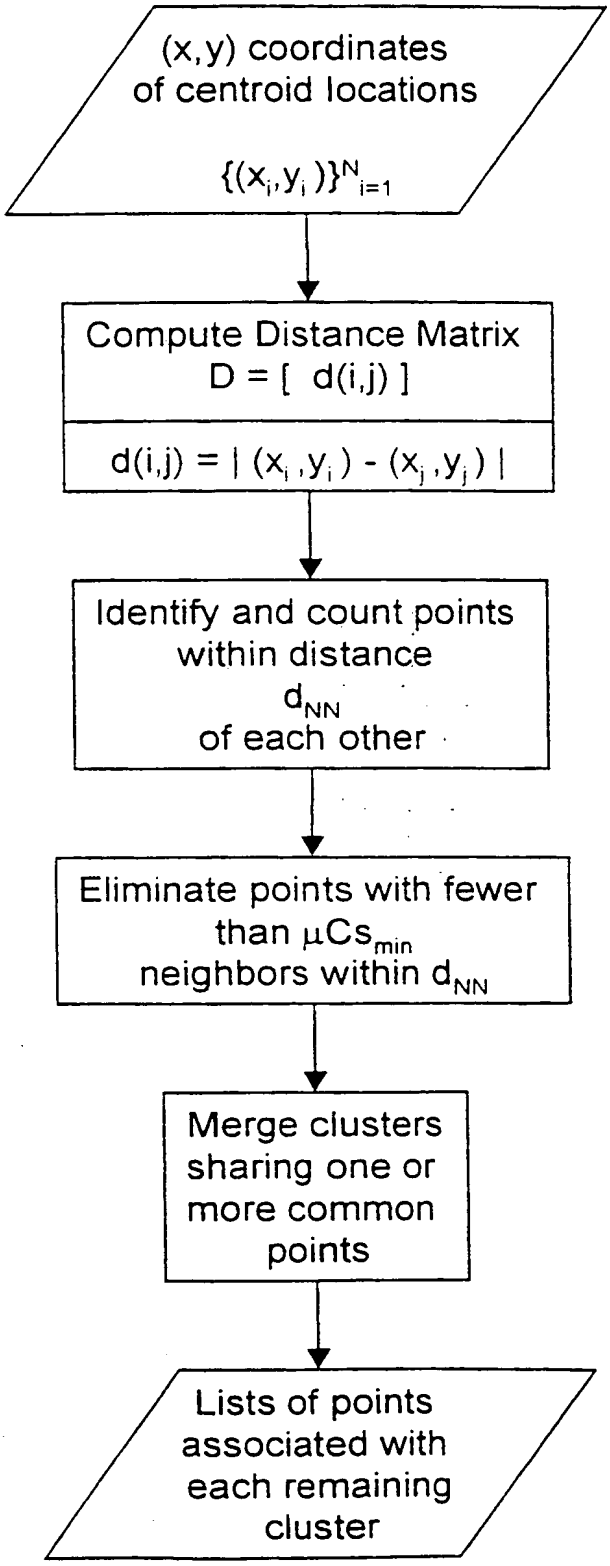
(x,y) coordinates of centroid locations
$\{(x_i,y_i)\}^N_{i=1}$
Compute Distance Matrix D = [d(i,j)]
$d(i,j) = |(x_i,y_i) - (x_j,y_j)|$
Identify and count points within distance d_{NN} of each other
Eliminate points with fewer than μCs_{min} neighbors within d_{NN}
Merge clusters sharing one or more common points
Lists of points associated with each remaining cluster

Fig. 20

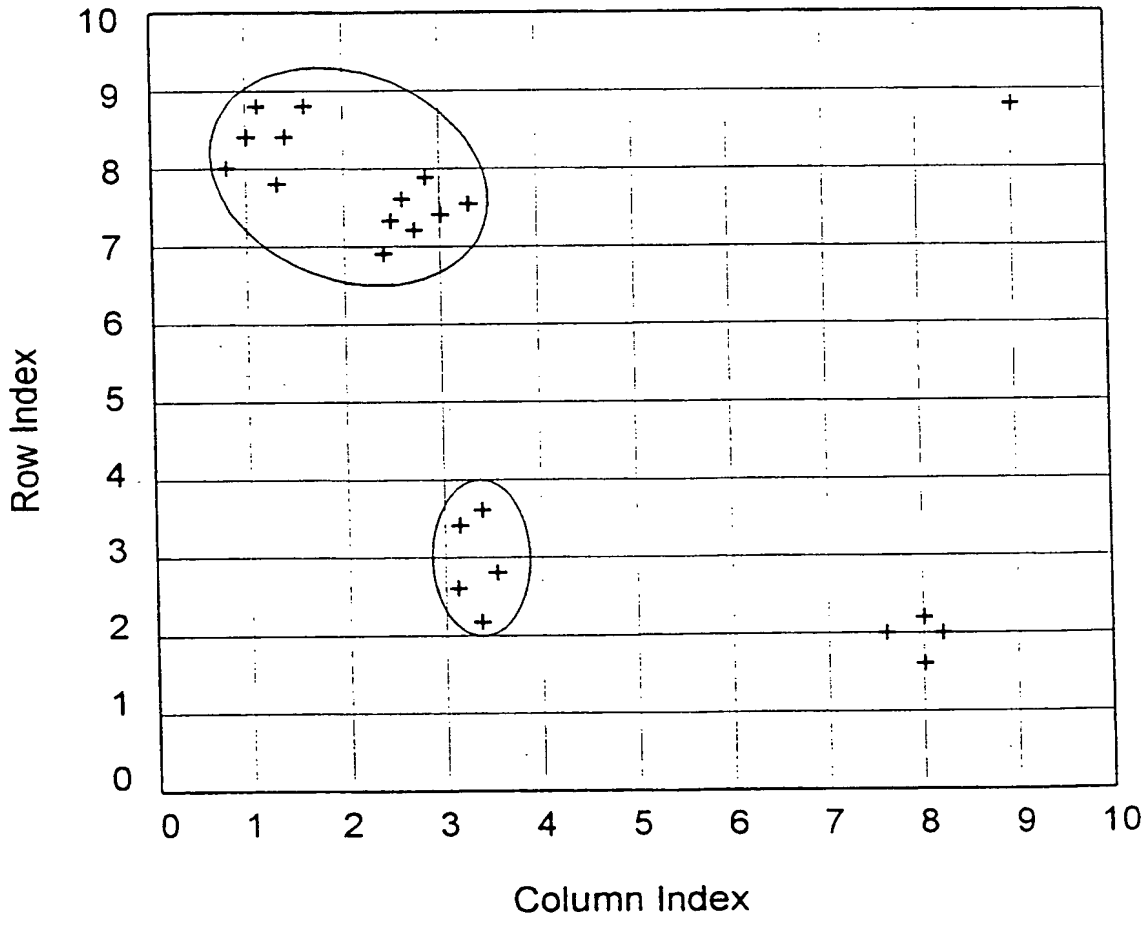

Fig. 21

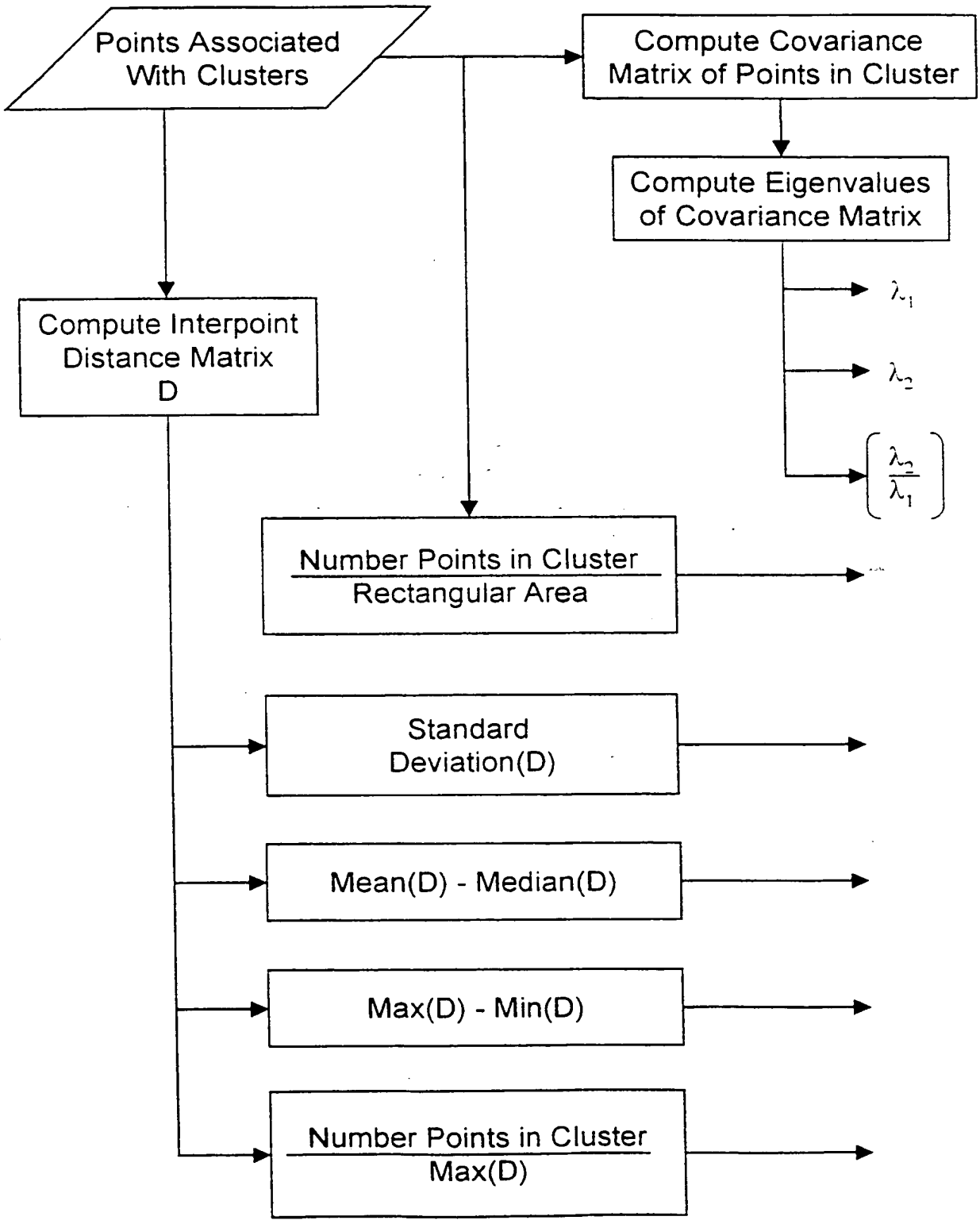
Points Associated With Clusters
Compute Covariance Matrix of Points in Cluster
Compute Eigenvalues of Covariance Matrix
λ_1
λ_2
$\frac{\lambda_2}{\lambda_1}$
Compute Interpoint Distance Matrix D
Number Points in Cluster / Rectangular Area
Standard Deviation(D)
Mean(D) - Median(D)
Max(D) - Min(D)
Number Points in Cluster / Max(D)

Fig. 22

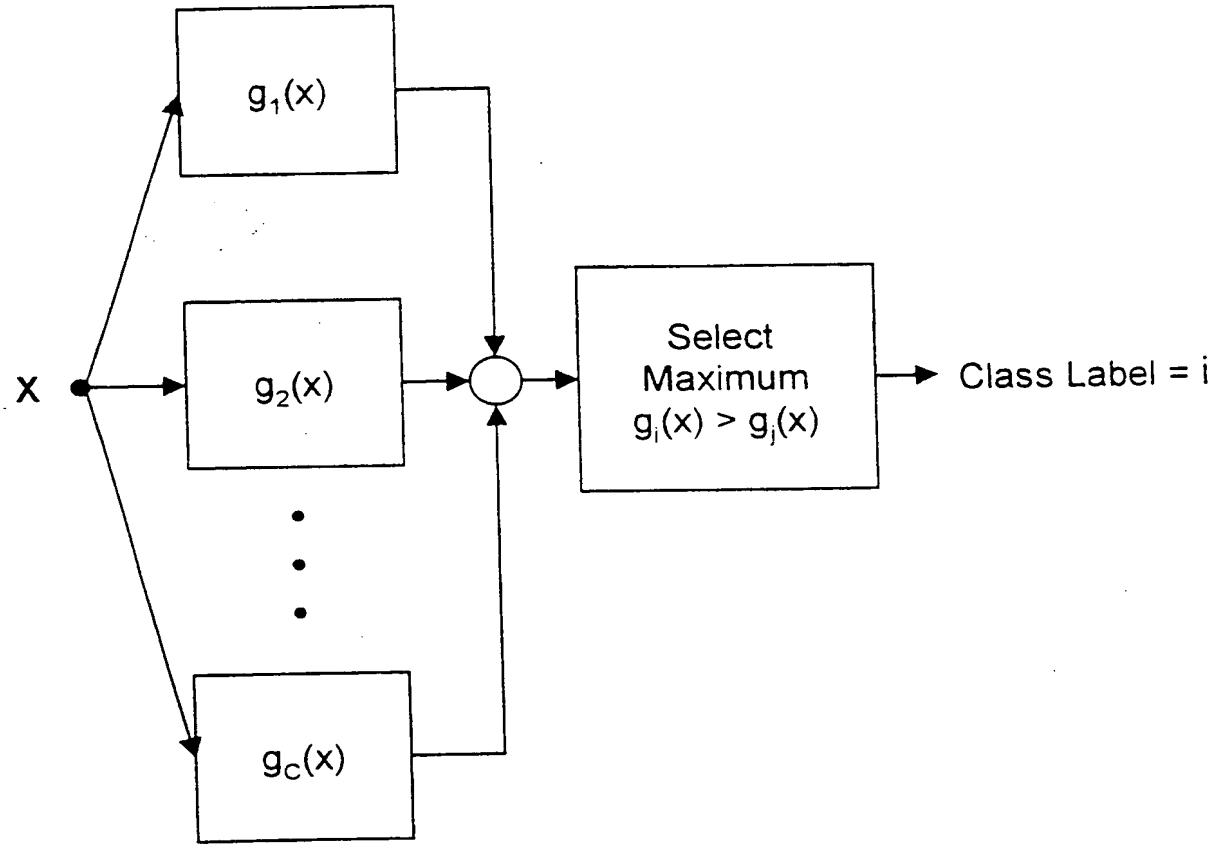

Fig. 23

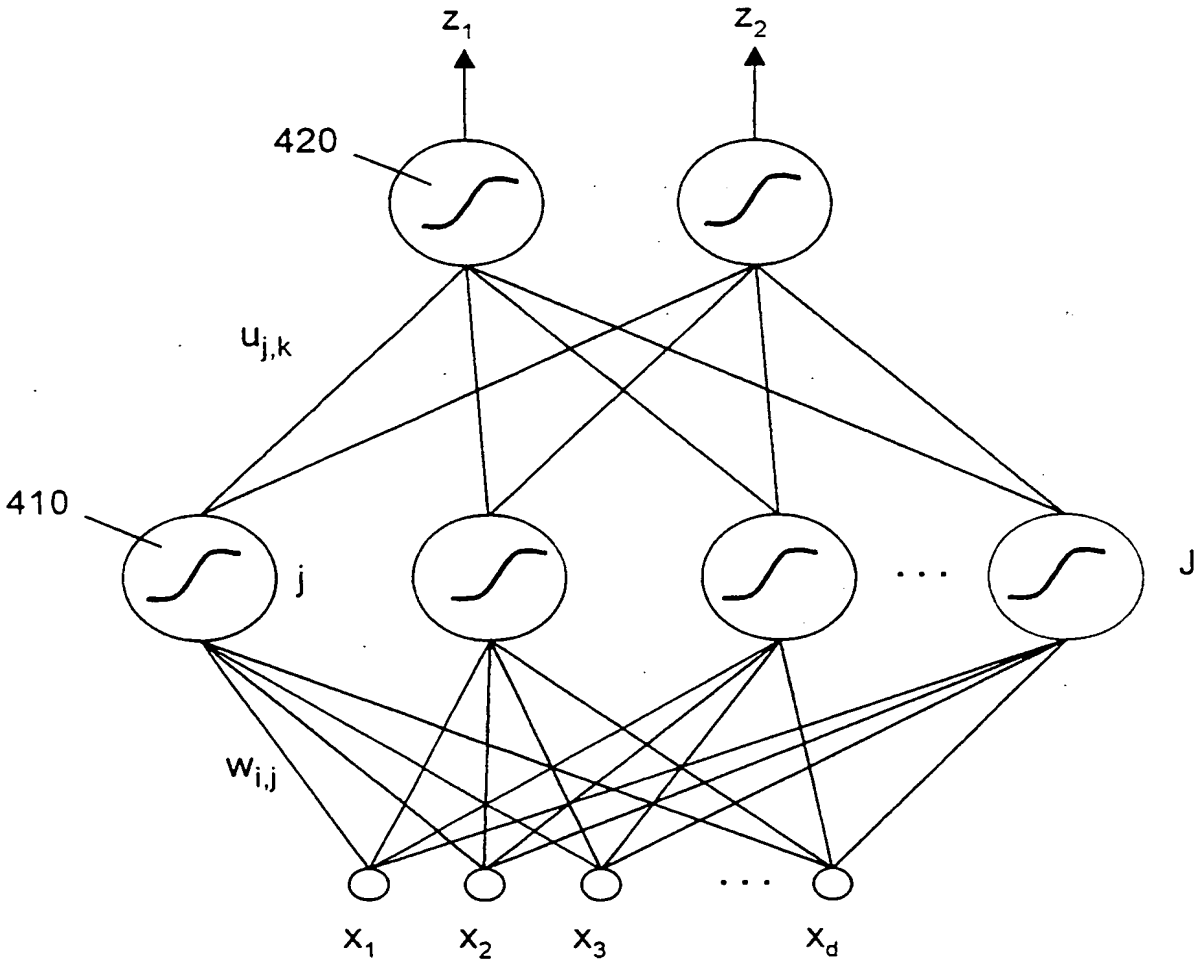

Fig. 24

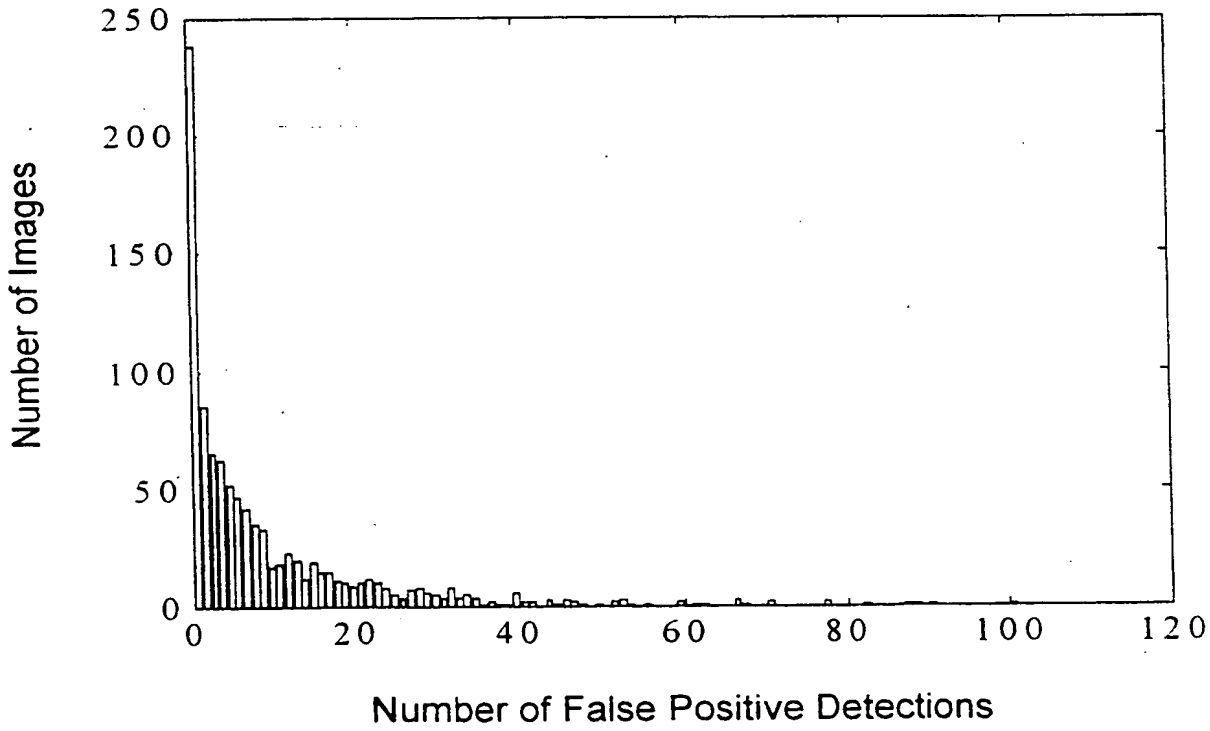
250
200
150
100
50
0
Number of Images
0
20
40
60
80
100
120
Number of False Positive Detections

Fig. 25

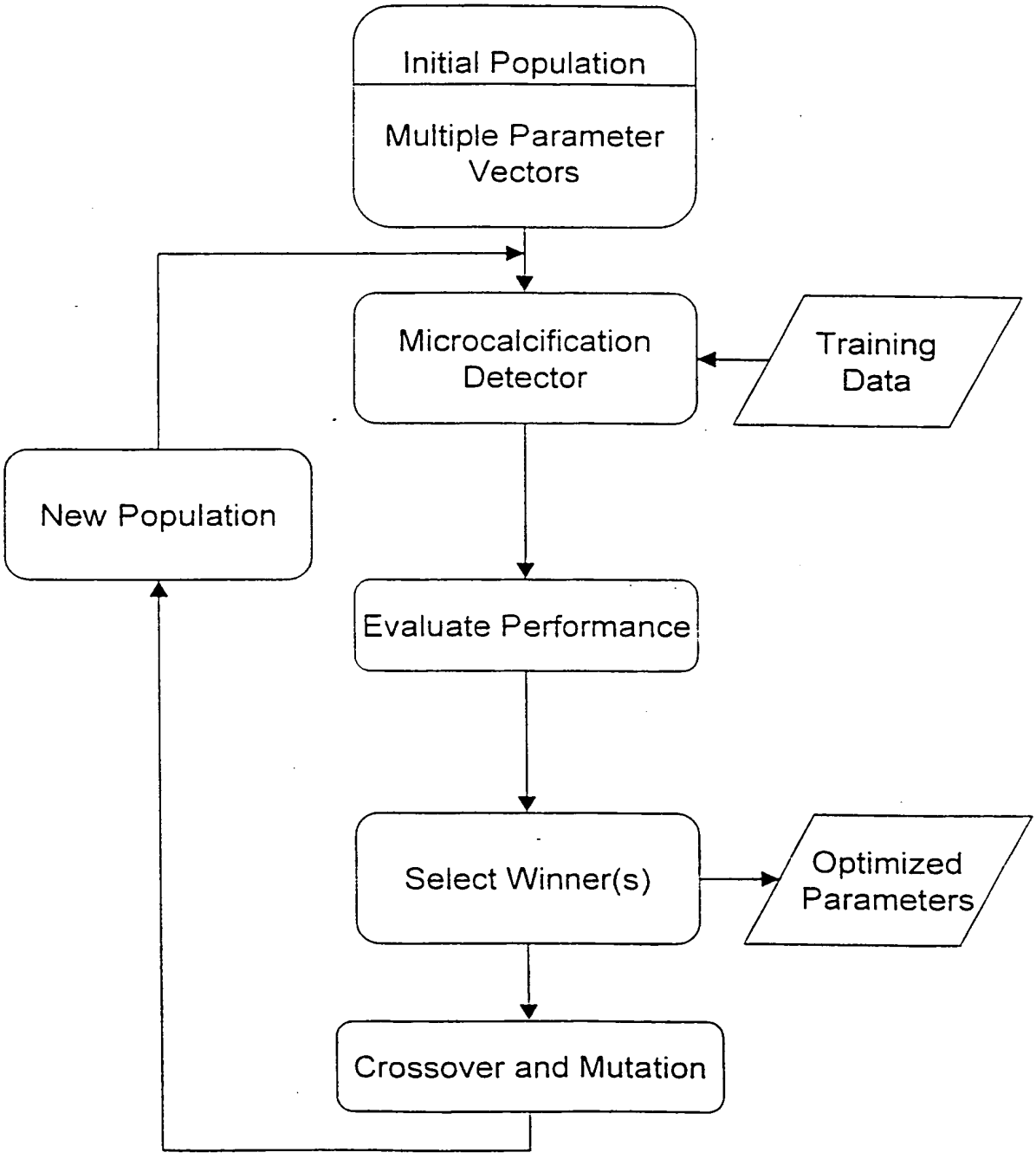
Initial Population
Multiple Parameter Vectors
Microcalcification Detector
Training Data
New Population
Evaluate Performance
Select Winner(s)
Optimized Parameters
Crossover and Mutation

Fig. 26

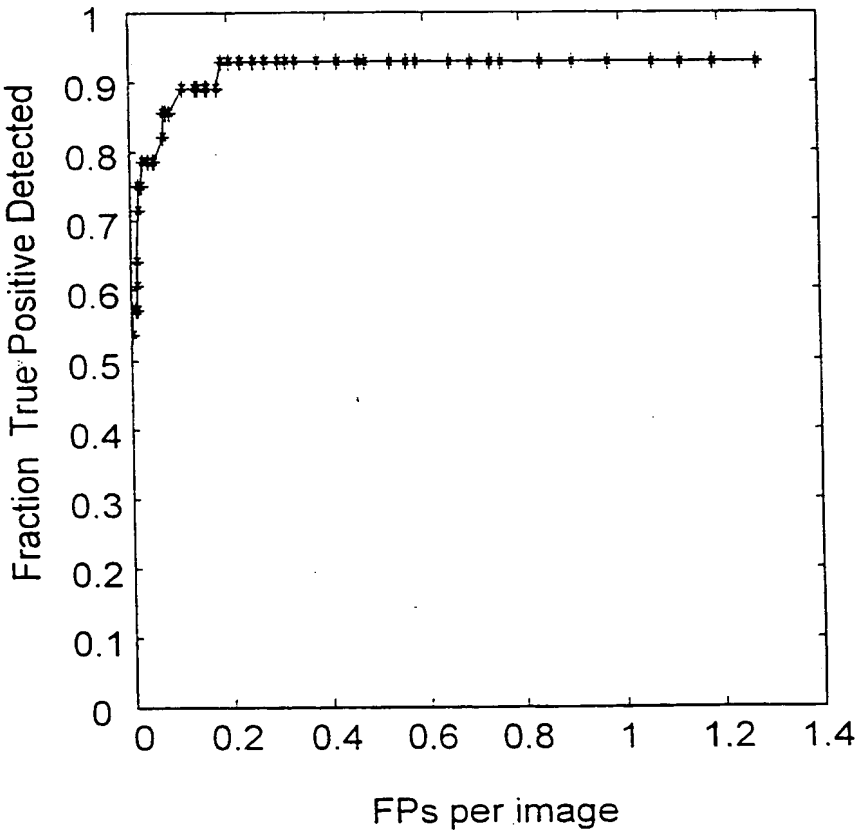
Fraction True Positive Detected
1
0.9
0.8
0.7
0.6
0.5
0.4
0.3
0.2
0.1
0
0
0.2
0.4
0.6
0.8
1
1.2
1.4
FPs per image

Fig. 27

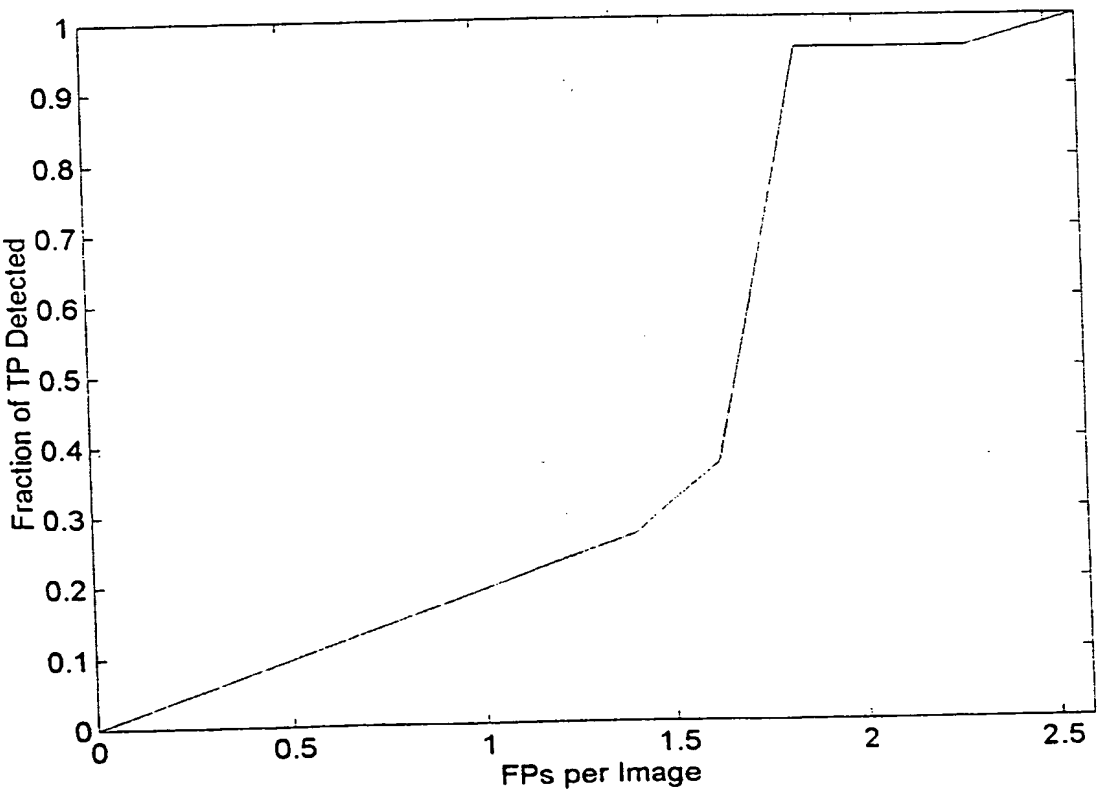
Fraction of TP Detected
FPs per Image
0
0.1
0.2
0.3
0.4
0.5
0.6
0.7
0.8
0.9
1
0
0.5
1
1.5
2
2.5

Fig. 28

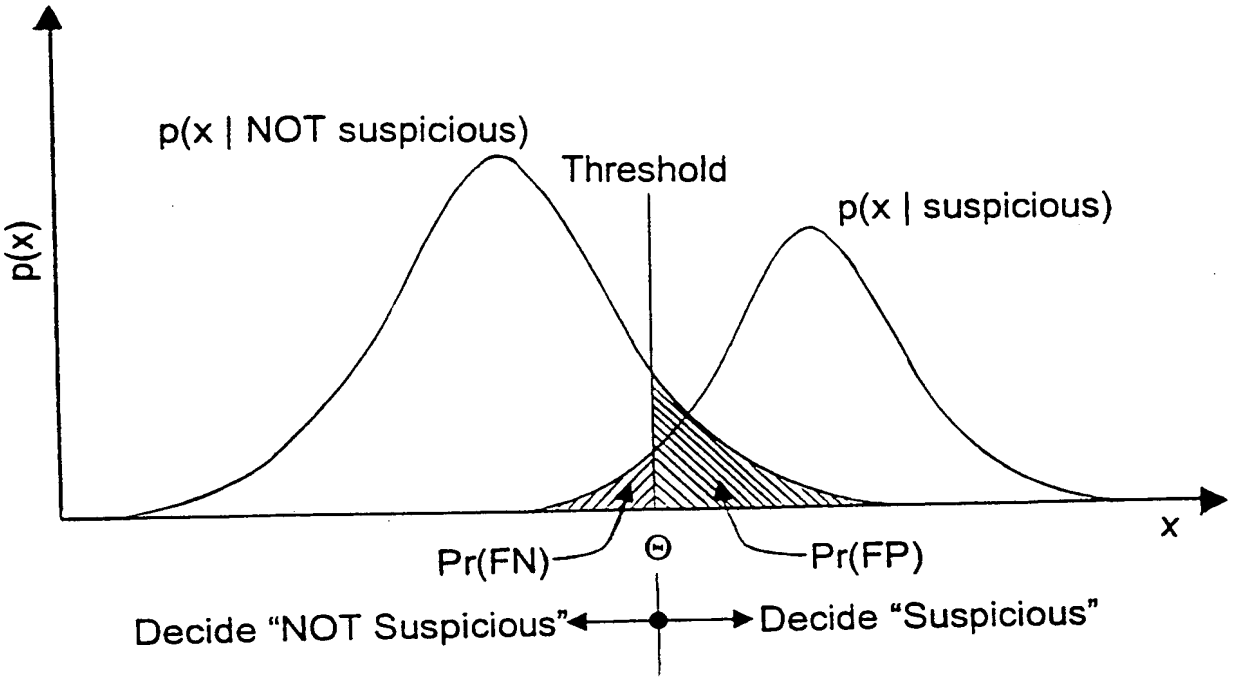
p(x | NOT suspicious)
Threshold
p(x | suspicious)
p(x)
x
Pr(FN)
Θ
Pr(FP)
Decide "NOT Suspicious"
Decide "Suspicious"

Fig. 29

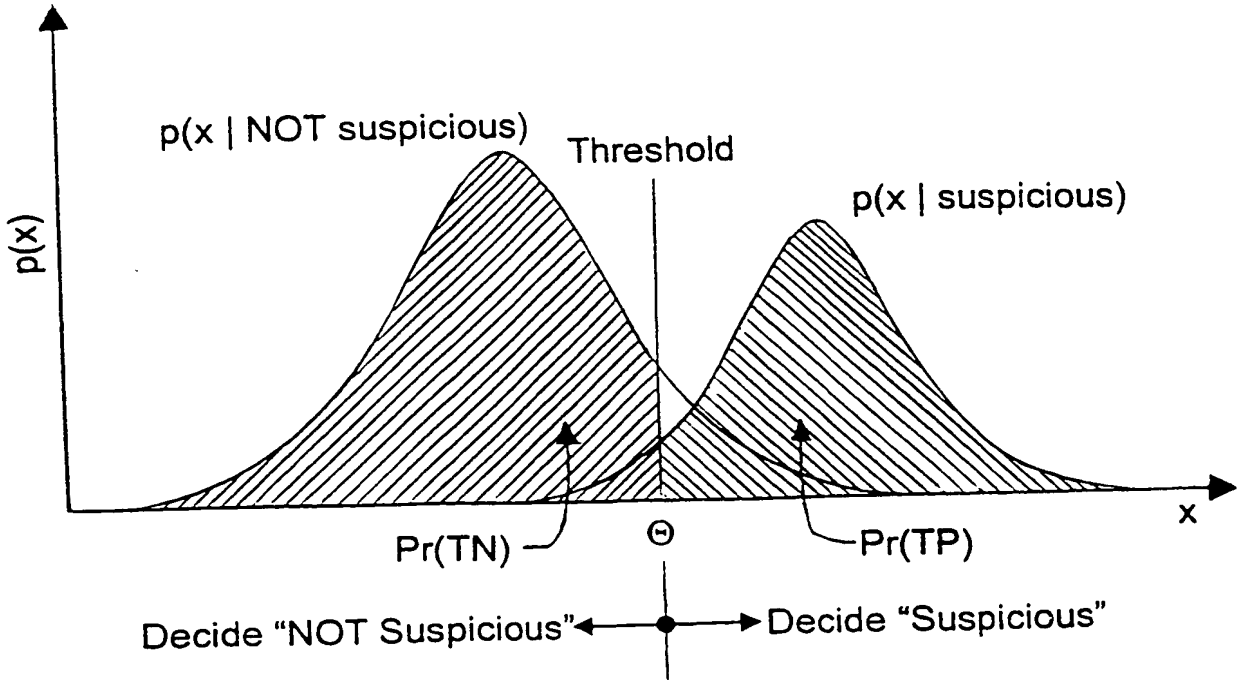
p(x | NOT suspicious)
Threshold
p(x | suspicious)
p(x)
x
Pr(TN)
Θ
Pr(TP)
Decide "NOT Suspicious"
Decide "Suspicious"

Fig. 30

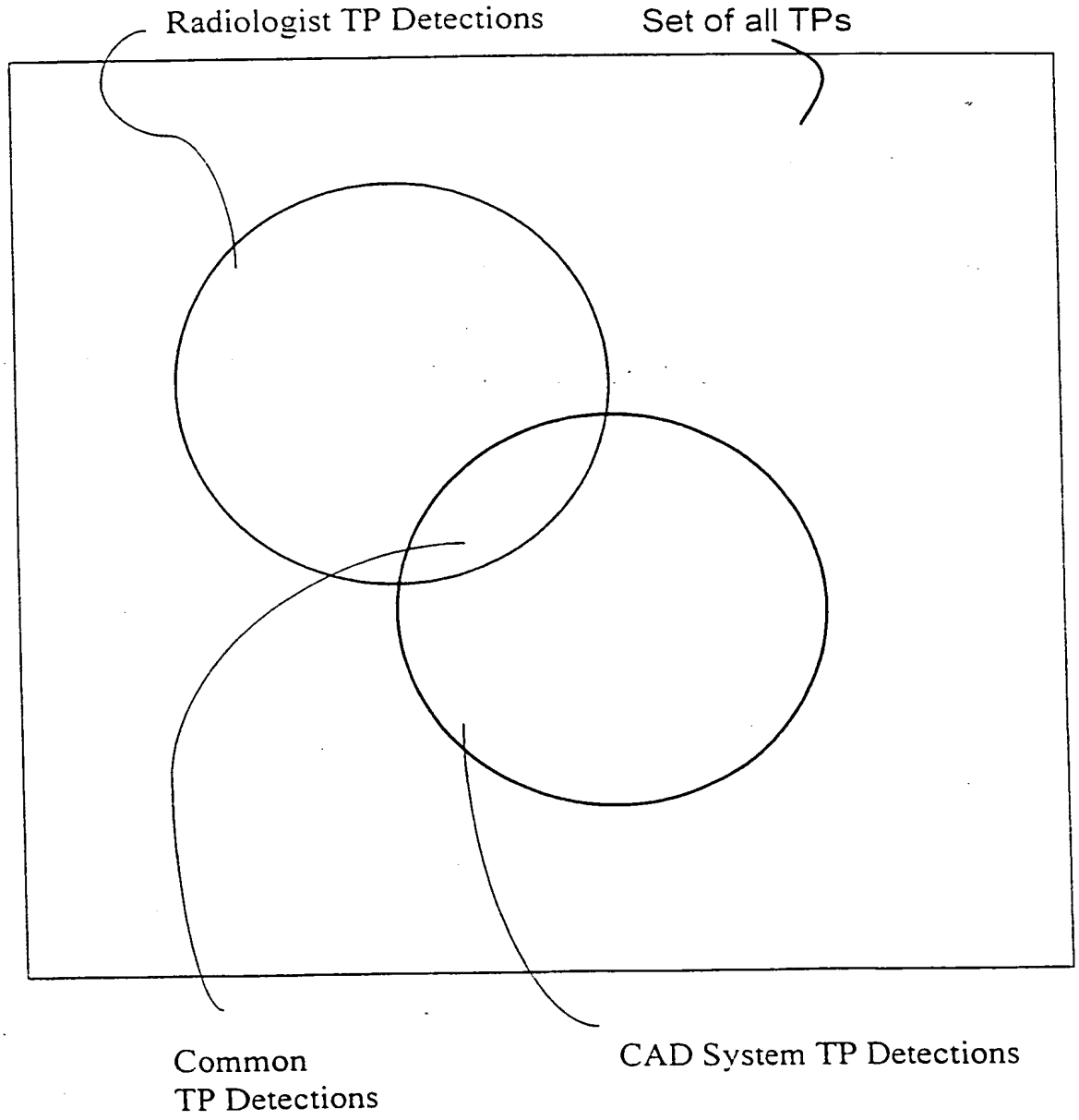
Radiologist TP Detections
Set of all TPs
Common
TP Detections
CAD System TP Detections

Fig. 31

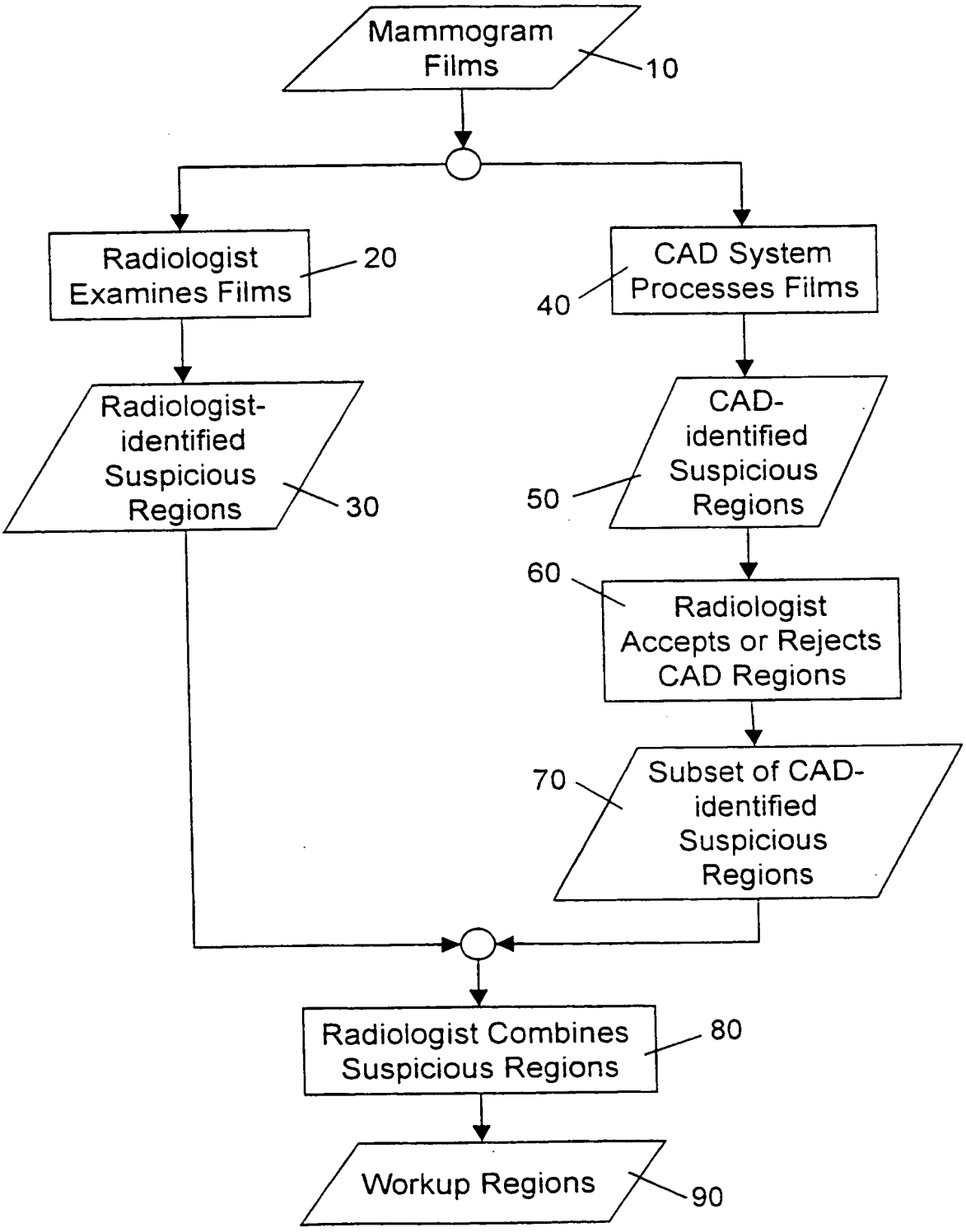
Mammogram Films
10
Radiologist Examines Films
20
CAD System Processes Films
40
Radiologist-identified Suspicious Regions
30
CAD-identified Suspicious Regions
50
60
Radiologist Accepts or Rejects CAD Regions
70
Subset of CAD-identified Suspicious Regions
Radiologist Combines Suspicious Regions
80
Workup Regions
90

Fig. 32

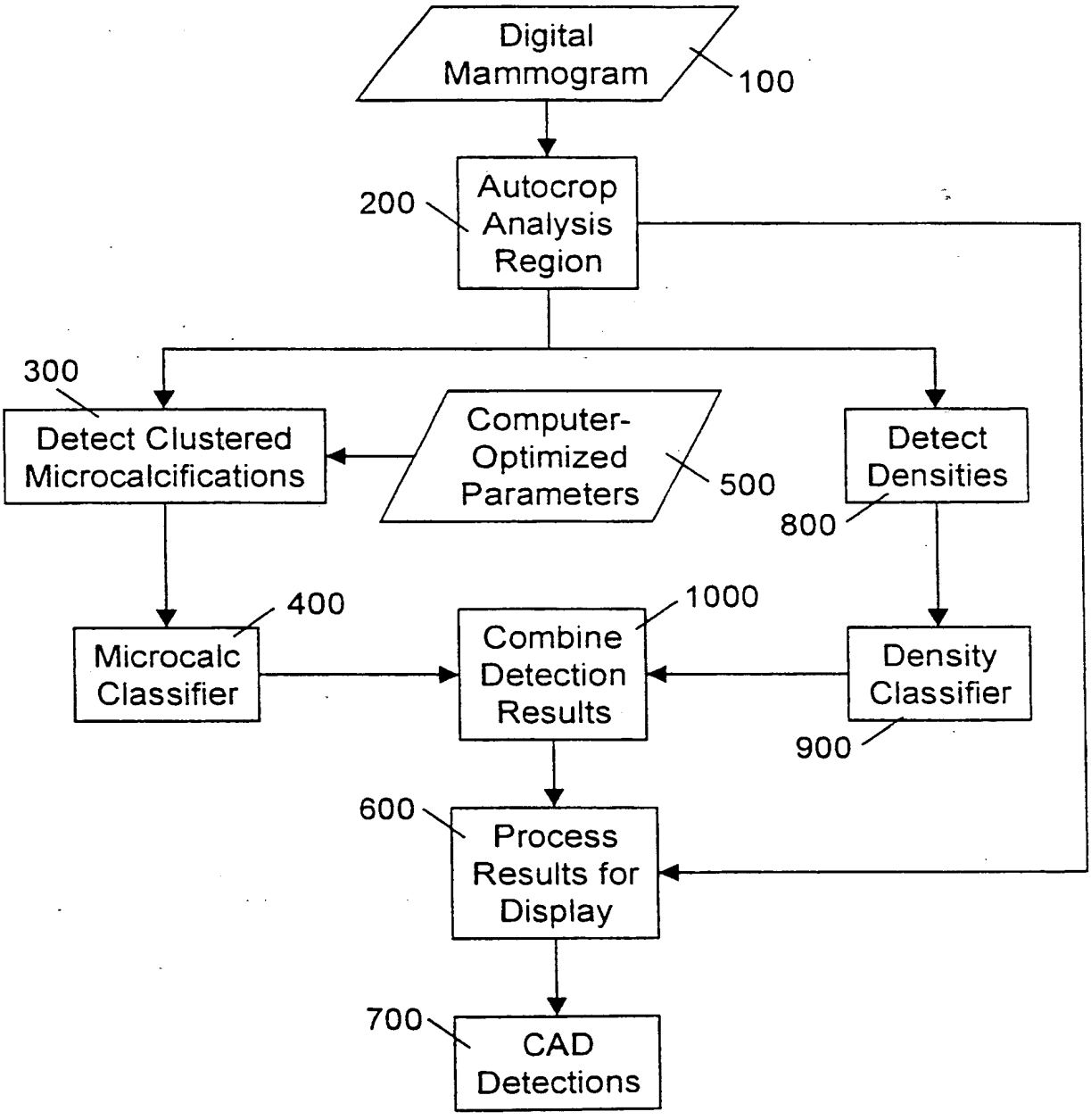
Digital Mammogram
100
200
Autocrop Analysis Region
300
Detect Clustered Microcalcifications
Computer-Optimized Parameters
500
Detect Densities
800
400
Microcalc Classifier
1000
Combine Detection Results
Density Classifier
900
600
Process Results for Display
700
CAD Detections

INTERNATIONAL SEARCH REPORT

International application No.
PCT/US98/17886

A. CLASSIFICATION OF SUBJECT MATTER

IPC(6) :A61B 6/00
US CL :128/922, 925; 382/128, 132; 600/407, 408

According to International Patent Classification (IPC) or to both national classification and IPC

B. FIELDS SEARCHED

Minimum documentation searched (classification system followed by classification symbols)

U.S. : 128/920, 922, 925; 378/37; 382/128, 132, 156, 159, 169-171; 600/407, 408

Documentation searched other than minimum documentation to the extent that such documents are included in the fields searched

Electronic data base consulted during the international search (name of data base and, where practicable, search terms used)

APS
Serch Terms: mammogram, digital, microcalcifications, crop, mask

C. DOCUMENTS CONSIDERED TO BE RELEVANT

Category*	Citation of document, with indication, where appropriate, of the relevant passages	Relevant to claim No.
X --- E Y	US 5,825,910 A (VAFAI) 20 October 1998, Abstract, Figs. 1 and 2, col. 1 lines 41-60, col. 2 lines 7-19, col. 3 lines 36-47, col. 5 lines 13-47, col. 6 lines 4-33, col. 8 lines 18-31, and claims 1-13.	1, 2, 5, 17, 18, 20, 28, 37, 38, 40, 41 --- 10-16, 23, 29-35
Y	US 5,622,171 A (ASADA et al.) 22 April 1997, Abstract, Figs. 1-13, col. 2 lines 8-44, col. 3 lines 12-18, col. 11 lines 33-63, and claims 1-26.	10-16, 23, 29-35

[X] Further documents are listed in the continuation of Box C. [ ] See patent family annex.

*	Special categories of cited documents:	"T"	later document published after the international filing date or priority date and not in conflict with the application but cited to understand the principle or theory underlying the invention
"A"	document defining the general state of the art which is not considered to be of particular relevance	"X"	document of particular relevance; the claimed invention cannot be considered novel or cannot be considered to involve an inventive step when the document is taken alone
"E"	earlier document published on or after the international filing date	"Y"	document of particular relevance; the claimed invention cannot be considered to involve an inventive step when the document is combined with one or more other such documents, such combination being obvious to a person skilled in the art
"L"	document which may throw doubts on priority claim(s) or which is cited to establish the publication date of another citation or other special reason (as specified)	"&"	document member of the same patent family
"O"	document referring to an oral disclosure, use, exhibition or other means		
"P"	document published prior to the international filing date but later than the priority date claimed		

Date of the actual completion of the international search 23 OCTOBER 1998	Date of mailing of the international search report 16 NOV 1998
Name and mailing address of the ISA/US Commissioner of Patents and Trademarks Box PCT Washington, D.C. 20231 Facsimile No. (703) 305-3230	Authorized officer SHAWNA J. SHAW Telephone No. (703) 308-2985

Form PCT/ISA/210 (second sheet)(July 1992)*

INTERNATIONAL SEARCH REPORT

International application No.
PCT/US98/17886

C (Continuation). DOCUMENTS CONSIDERED TO BE RELEVANT

Category*	Citation of document, with indication, where appropriate, of the relevant passages	Relevant to claim No.
X	US 5,491,627 A (ZHANG et al.) 13 February 1996, Abstract, Figs. 1-19, col. 1 lines 40-62, col. 2 lines 20-57, col. 5 lines 9-20, col. 9 line 16 to col. 10 line 21, col. 17 lines 23-67, col. 18 lines 1-23, and claims 1-48.	1, 2, 5-20, 23-42, 44, 45, 47-51
A	US 5,572,565 A (ABDEL-MOTTALEB) 05 November 1996, Abstract, Figs. 1-4, col. 2 lines 3-43, and claims 1-3.	1-51

THIS PAGE BLANK (USPTO)